

**DRY PURIFICATION OF ETHANOLIC BIODIESEL
PRODUCED FROM WASTE COOKING OILS THROUGH
ADSORPTION PROCESSES**

Camilla Groxko Smolich

Thesis presented to the Escola Superior de Tecnologia e Gestão of the Instituto Politécnico de Bragança to obtain the Master's Degree in Chemical Engineering within the scope of the double diploma with the Universidade Tecnológica Federal do Paraná, Campus Apucarana

Supervised by

Paulo Miguel Pereira de Brito
Ana Maria Alves Queiroz da Silva
António Manuel Esteves Ribeiro
Maria Carolina Sérgi Gomes

BRAGANÇA

February 2024

AGRADECIMENTOS

Agradeço primeiramente a Deus, pois foi quem me possibilitou chegar até aqui. Aos meus orientadores Professor Doutor Paulo Brito, Professora Doutora Ana Queiroz, Professor Doutor António Ribeiro e à Professora Doutora Maria Carolina Sérgi Gomes pela orientação e pelo apoio.

Agradeço ao Instituto Politécnico de Bragança e à Universidade Tecnológica Federal do Paraná pela oportunidade de realizar esse intercâmbio de estudos e aos professores que foram essenciais durante a minha formação como Engenheira Química. Ao LAMAP e à Dra. Maria João pelo auxílio no decorrer da pesquisa.

Agradeço à minha família que me apoiou, especialmente aos meus pais e à minha irmã, Mônica, Glen e Milena, por todo o suporte durante a minha formação, por me incentivarem a me tornar uma excelente profissional e sempre buscar meus sonhos. Ao Lucas Carvalho que me deu forças, me encorajou e sempre esteve lá por mim durante esse processo, mesmo de longe. À Maísa que se tornou uma verdadeira irmã para mim. Aos meus colegas de pesquisa Miriam, João, Tairone, Lariane, Caio, Raphaela, Eduardo, Maria e Gabriel que se tornaram verdadeiros amigos e que me acompanharam nos momentos bons e ruins, sempre deixando tudo mais leve.

ABSTRACT

Due to the risk of possible depletion of fossil fuels and the increasing consumption of energy from renewable energy sources, biodiesel emerges as an alternative to non-renewable fuel. An important stage in its production process is purification, commonly done through wet washing to remove glycerol in solution. However, this method consumes large volumes of water, resulting in significant effluent volumes. Therefore, this study aimed to apply adsorption as an alternative method.

To apply this method, the chosen agroindustrial waste was olive pit, as it is widely produced in Portugal and was implemented in the form of activated carbon. The overall process involved three main stages: biodiesel and activated carbon production, subsequent characterization, and adsorption tests for glycerol removal.

Biodiesel was produced through transesterification of waste cooking oil under specific conditions, resulting in a sample with high glycerol content, incomplete conversion to fatty acid esters, and high in linoleic acid ethyl ester, indicating the presence of sunflower oil.

The activated carbon was produced from dry olive pits and showed basic characteristics, suitable for glycerol removal. Adsorption kinetic tests revealed that the activated carbon was favorable in removing glycerol from the biodiesel, with the best result achieved at 25°C after 1440 minutes, reaching 89.7% glycerol removal.

The isotherm models used in the study showed favorable results, indicating that adsorption occurred in a multilayer formation and on a heterogeneous surface. However, the study concluded that while the activated carbon contributes to biodiesel purification, it cannot completely substitute wet washing due to the inability to achieve the required glycerol content limit in a single stage process. In the future, other conditions may be added to this work, for example: use different kinds of WCO, different activations of the adsorbent, different transesterification conditions, recycle AC, and change the purification from batch to continuous process.

The study's results provide valuable insights into the potential of olive pits activated carbon for biodiesel purification and the limitations of its use as a complete substitute for wet washing.

Keywords: Biodiesel purification, adsorption, dry washing; waste cooking oil; olive pits activated carbon.

RESUMO

Devido ao risco de possível esgotamento de combustíveis fósseis e ao aumento de consumo de energia de energias de fontes renováveis, o biodiesel surge como uma alternativa para os combustíveis de fontes não-renováveis. Uma importante etapa para o seu processo de produção é a purificação, comumente feita por lavagens aquosas, a fim de remover o glicerol em solução. Entretanto, esse método consome grandes volumes de água, gerando assim grandes volumes de efluente. Dessa forma, este estudo teve como objetivo aplicar a adsorção como método alternativo.

Para aplicar este método, o resíduo agroindustrial escolhido foi o caroço de azeitona, uma vez que é amplamente produzido em Portugal e foi implementado na forma de carbono ativado. O processo global envolveu três etapas principais: produção de biodiesel e de carvão ativado, posterior caracterização e testes de adsorção para remoção do glicerol.

O biodiesel foi produzido por transesterificação de óleo residual alimentar, resultando em uma amostra com alto teor de glicerol, conversão incompleta em ésteres de ácidos graxos e alto teor de ésteres etílicos de ácido linoleico, indicando a predominância de óleo de girassol.

O carbono ativado foi produzido a partir de caroços secos de azeitona e apresentou características básicas, adequadas para a remoção de glicerol. Testes cinéticos de adsorção revelaram que o carbono ativado foi favorável na remoção de glicerol do biodiesel, com o melhor resultado alcançado, 89.7 % de remoção, a 25 °C após 24 h.

Os modelos de isotérmicas de Freundlich, Langmuir e BET usados no estudo mostraram resultados favoráveis, indicando que a adsorção ocorreu em multicamada e em uma superfície heterogênea. No entanto, o estudo permitiu concluir que, embora o adsorvente preparado contribua para a purificação do biodiesel, ele não pode substituir completamente a lavagem húmida devido à incapacidade de atingir o limite de teor de glicerol requerido com um processo de passo único. No futuro, outras condições podem ser adicionadas, como por exemplo: usar diferentes tipos de óleo residual de cozinha, diferentes ativações do adsorvente, diferentes condições de transesterificação, reciclar o carbono ativado e mudar o processo de batelada para contínuo.

Os resultados do estudo fornecem informações valiosas sobre o potencial do carvão ativado do caroço de azeitona para a purificação do biodiesel e as limitações de seu uso como substituto completo para a lavagem húmida.

Palavras-chave: Purificação de biodiesel, adsorção, lavagem a seco, óleo residual, carbono ativado de caroço de azeitona.

Table of Contents

LIST OF FIGURES	ix
LIST OF TABLES	x
NOMENCLATURE AND SYMBOLS	xi
1. BACKGROUND	1
2. BIODIESEL	3
2.1 FEEDSTOCK	4
2.1.1 Waste cooking oil	6
2.2 BIODIESEL PRODUCTION	6
2.2.1 Pyrolysis	7
2.2.2 Esterification	7
2.2.3 Transesterification	7
2.3 CATALYST	8
2.4 PURIFICATION	11
2.4.1 Wet washing	11
2.4.2 Centrifugation.....	11
2.4.3 Membrane filtration.....	12
2.4.4 Dry washing	12
2.5 ADSORPTION.....	13
2.5.1 INFLUENCING FACTORS	14
2.5.1.1 Surface area	14
2.5.1.2 Temperature.....	14
2.5.1.3 pH.....	15
2.6 ADSORBENTS.....	15
2.7 KINETICS	16
2.7.1 Activation energy	17
2.8 ISOTHERMS	18
2.8.1 Freundlich.....	19

2.8.2 Langmuir	20
2.8.3 Linear.....	20
2.8.4 BET	20
3. METHODOLOGY	22
3.1 REACTANTS	22
3.2 EQUIPMENT	22
3.3 WCO CHARACTERIZATION	22
3.3.1 WCO acidity.....	22
3.3.2 Density.....	23
3.4 BIODIESEL PRODUCTION.....	23
3.4.1 Glycerol quantification.....	24
3.4.2 Fatty acid ethyl ester (FAEE) yield.....	25
3.5 ADSORBENT PREPARATION	25
3.5.1 Granulometry.....	26
3.5.2 pH _{PZC}	26
3.5.3 Fourier Transform Infrared Spectroscopy (FTIR).....	27
3.5.4 Surface composition	27
3.5.5 Thermogravimetry (TGA)	28
3.6 ADSORPTION STUDIES	28
3.6.1 Kinetic study.....	28
3.6.2 Equilibrium study	28
4. RESULTS AND DISCUSSION.....	29
4.1 OIL AND BIODIESEL CHARACTERIZATION.....	29
4.1.1 FAEE content and reaction yield.....	29
4.2 ADSORBENT CHARACTERIZATION.....	30
4.2.1 Granulometry.....	31
4.2.2 pH _{PZC} and functional groups	31
4.2.3 Thermogravimetry (TGA)	33

4.3 PURIFICATION THROUGH ADSORPTION	33
4.3.1 Kinetics.....	33
4.3.2 Activation energy	36
4.3.3 Isotherm.....	37
5. CONCLUSIONS	40
REFERENCES	42
APPENDIX A – CALIBRATION CURVES.....	51
APPENDIX B – FAME IDENTIFICATION.....	53
APPENDIX C – SCIENTIFIC PRESENTATION	54

LIST OF FIGURES

Figure 1: Percentage of global primary energy between 1995 and 2020.	3
Figure 2: Esterification reaction.	7
Figure 3: Transesterification reaction.	8
Figure 4: Isotherm typical behaviors.	19
Figure 5: Biodiesel production through transesterification.	24
Figure 6: Biodiesel FAEE characterization.	29
Figure 7: a) Crude olive pits, b) ground olive pits and c) OPAC.	30
Figure 8: FTIR spectrum of olive pits before and after carbonization.	32
Figure 9: Thermogravimetry for OPAC.	33
Figure 10: Kinetic study at 25, 35 and 45 °C with 5 wt% adsorbent.	34
Figure 11: Glycerol content throughout the kinetic study.	34
Figure 12: Glycerol concentration on the adsorbent vs time using 5 wt% OPAC at a) 25 °C, b) 35 °C and c) 45 °C using pseudo-first and pseudo-second order models.	36
Figure 13: Isotherm experimental data at 25 °C.	38
Figure 14: Isotherm experimental data at 25 °C and linear, Freundlich, Langmuir and BET models.	39

LIST OF TABLES

Table 1: Growth rate of biodiesel consumption in Brazil, Canada and Mexico and Europe in thousand barrels per day between 2009 and 2019.....	4
Table 2: Major producers of oilseed in the world.	5
Table 3: Properties of popular biodiesel feedstock.	5
Table 4: Catalysts used in biodiesel production and yield through transesterification. .	10
Table 5: Comparison of biodiesel purification methods.	13
Table 6: Biomass as adsorbent and its effect in biodiesel purification.	16
Table 7: Adsorbents preparation and specific area.....	16
Table 8: Methyl/ethyl esters identification in biodiesel before purification.	30
Table 9: Granulometric particle size distribution.	31
Table 10: AC characterization.....	31
Table 11: Peaks noticed through FTIR and their respective functional group.....	32
Table 12: Pseudo-first and pseudo-second order parameters for kinetic studies at 25, 35 and 45 °C with OPAC concentration equal to 5 %.	35
Table 13: Activation energy values for pseudo-first and pseudo-second order.	37
Table 14: Glycerol content after equilibrium at 25 °C for each AC concentration.....	37
Table 15: Freundlich, Langmuir, linear and BET model parameters for the 25 °C isotherm.	38

NOMENCLATURE AND SYMBOLS

AC	Acid value	mg of KOH/g
A	Pre-exponential factor	
C ₀	Initial adsorbate concentration in the liquid	wt%
C _e	Adsorbate concentration in the liquid at equilibrium	wt%
C _{KOH}	Concentration of standard solution	mol/L
E _a	Activation Energy	kJ/mol
k	Kinetic constant	
k ₁	Pseudo-first order constant	min ⁻¹
k ₂	Pseudo-second order constant	g/(mg.min)
K _F	Freundlich equilibrium constant	(mg/g).(mg/g) ^{-1/n}
K _L	Langmuir equilibrium constant	g/mg
K _S	Equilibrium constant for multilayer adsorption	g/mg
m _b	Biodiesel mass	g
m _a	Adsorbent mass	g
MM _{KOH}	Molar mass of KOH	g/mol
m _{oil}	Oli mass	kg
m _{sample}	Sample mass	g
m _{water}	Water mass	kg
n	Dimensionless exponent in the Freundlich model	
q _e	Mass of adsorbate removed by the adsorbent at equilibrium	mg/g
q _t	Adsorbate concentration removed by the adsorbent	mg/g
Q _{max}	Maximum adsorption capacity	mg/g
R	Ideal gas constant	J/(mol.K)
T	Temperature	K
ρ _{oil,water}	Relative density between oil and water	kg/m ³
ρ _{oil}	Oil density	kg/m ³
ρ _{water}	Water density	kg/m ³
V _{al}	Aliquot volume	L
V _b	Volume used to titrate the blank solution	L
V _{KOH}	Volume of titrant solution	mL

$V_{\text{pycnometer}}$	Volume of pycnometer	mL
V_{sam}	Sample volume	L
V_{T}	Volume of the initial solution	L
AC	Activated Carbon	
CNPE	National Energy Policy Council	
EU	European Union	
FAEE	Fatty Acid Ethyl Ester	
FAME	Fatty Acid Methyl Ester	
FFA	Free Fatty Acid	
FTIR	Fourier Transform Infrared Spectroscopy	
GC-FID	Gas Chromatography with Flame Ionization Detector	
OPAC	Olive Pit Activated Carbon	
pH	Potential of Hydrogen	
PNPB	National Program of Production and Use of Biodiesel	
USA	United States of America	
WCO	Waste Cooking Oil	

1. BACKGROUND

The need to study biofuel and renewable energy sources has increased due to the possible depletion of petroleum-based fuels and non-renewable sources such as natural gas. Parallel to this problem, the use of these fuels in transportation, industrial and domestic purposes produce high amounts of carbon dioxide in the atmosphere which increases air pollution and greenhouse gas effects [1].

In the meantime, efforts are being made to reduce dependence on petroleum and transition to more sustainable energy sources, such as wind, sunlight, and biofuels [2]. One of the most promising alternative fuels is biodiesel due to its renewable source and its ability to serve as a replacement for petro-diesel without the need for alterations in machines with combustion motors. Biodiesel also presents advantages over diesel fuel in terms of sulfur content, biodegradability, low sulfur content, flash point, no aromatic content, higher cetane number and miscibility in petroleum diesel in any ratio [3][4].

The production method most used of biodiesel is transesterification which involves the conversion of triglycerides into fatty acids alkyl esters after reacting with short-chain alcohols in the presence of a catalyst [5]. The source of triglycerides can be algae, animal fat, vegetable oils, etc. Moreover, the use of materials such as waste cooking oil (WCO) adds to the global reduction of residue, lowers the cost of production, and contributes to a circular economy [6]. Also, an important part of the production is purification, and the most used method is the wet washing step, where great amounts of water are mixed with biodiesel to remove glycerol. This step is due to the high solubility in water of glycerol and impurities present in the biofuel [2].

This work aims to produce biodiesel from sustainable and renewable sources such as WCO, and using an alternative purification method based on adsorption which generates less quantity of effluents as a result of the process. The study will be developed in order to determine the best conditions for the adsorption process in batch reactions and applying organic waste as adsorbent. The specific goals are:

- Produce ethylic biodiesel using WCO and the conditions studied in previous works, such as oil/alcohol molar ratio, temperature, and catalyst load.
- Use activated carbon produced from olive pits to purify the biodiesel through adsorption.

- Establish the best conditions for glycerol removal to biodiesel content values lower than 0.02 wt% in batch reactions and determine the adsorbent's maximum adsorption capacity.

2. BIODIESEL

According to the multinational energy company, BP, and its Statistical Review of World Energy in 2021, the shares of global primary energy are shown in Figure 1. As seen, oil (31.5 %) and coal (21.2 %) remain as the largest shares of the energy mix, whereas the shares of natural gas and renewables rose since 1995 to 24.7 % and 5.7 %, respectively. Nuclear energy (4.3 %) is now the least used and hydroelectricity (6.9 %) has shown little growth. Even though biodiesel is made of renewable sources such as vegetable oil, it is considered an oil along with petroleum and coal derivatives. As viewed on the graph, this type of energy remains the main one globally [7].

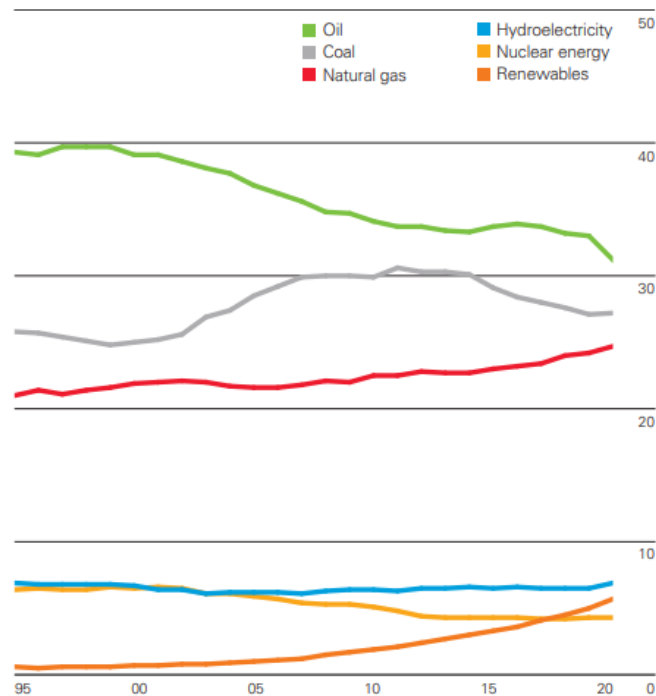


Figure 1: Percentage of global primary energy between 1995 and 2020.
Source: [7].

The same report shows that biodiesel growth rate consumption has increased in several emerging countries and in Europe, such as seen on Table 1. In total, biodiesel growth rate between 2009 and 2019 was 11.1 % [7].

Table 1: Growth rate of biodiesel consumption in Brazil, Canada and Mexico and Europe in thousand barrels per day between 2009 and 2019.

Country	Biodiesel consumption growth rate (Thousand barrels per day)
Brazil	14.2 %
Canada and Mexico	28.0 %
Europe	5.6 %

Source: [7].

In Europe, the Renewable Energy Directive stimulates the development of renewable energy sources to reduce greenhouse gas emissions by at least 55% by the year 2030 and to become a climate-neutral continent by 2050 [8]. Also, the REPowerEU Plan was created with the goal to lower energy dependence of Russia due to the war that began in the same year. For that matter, it sets actions such as saving energy, diversifying supplies, and to quickly substitute fossil fuels with clean energy [9].

Emerging countries such as Brazil and India have a high production of renewable energy sources, mainly ethanol due to plantations of sugar cane. Exportation numbers have increased to their maximum in 2022, little over 17,208 tons, the greatest number since 2014 [10, 11]. As for European countries, Portugal represents one of European nations with highest renewable sources ratio, since its electricity during 2023 was mostly supplied by renewable energy sources, increasing 49 % compared to electric energy supply in the previous year [12].

2.1 FEEDSTOCK

Biodiesel feedstock differs in each country depending on oilseed production, availability, climate, oil content and conversion rate. For instance, European countries use rapeseed and sunflower oil, whereas USA and Canada use corn, canola, and soybean oil and Brazil uses soybean and animal fat [13, 14]. Animal fat is used preferably in warmer climate countries due to its solidifying point. Table 2 presents the most produced oilseeds in several countries with potential to serve as biodiesel feedstock.

Table 2: Major producers of oilseed in the world.

Oilseed	Producing regions
Soybean	USA
	Brazil
	China
	Russia
	India
Sunflower	EU countries
	Ukraine
	Russia
	Argentina
Rape	EU countries
Cotton	USA
	Brazil
	China
Safflower	China
	USA
	Spain
	Portugal

Source: Adapted [13, 15].

Table 3 shows different physicochemical properties for various feedstocks that have been studied in biodiesel production, such as palm, soybean, sunflower, rapeseed, corn, cottonseed, and waste cooking oil. The purpose of studies involving feedstock is to find one with higher conversion rate into ester, greater efficiency in engines evaluating performance, gas emission and combustion behavior among edible and non-edible oils, and low production cost [13, 16].

Table 3: Properties of popular biodiesel feedstock.

Feedstock	Oil content (%)	Edible (E) or Non-edible (N)	Kinematic viscosity (mm²/s)	Density (kg/m³)	Higher heating value (MJ/kg)	Flash point (°C)	Cetane number
Palm	30-60	E	40.33	913.90	40.80	275	42.0
Soybean	15-22	E	32.60	913.80	37.30	254	37.9
Sunflower	25-35	E	37.10	916.10	39.60	274	37.1
Rapeseed	38-46	E/N	36.30	906.20	39.70	246	37.6
Corn	20	E	34.90	909.50	39.50	277	37.6
Cottonseed	18-25	N	33.50	914.80	39.50	234	41.8
Waste cooking oil	-	N	45.35	918.40	35.82	236	30.0

Source: Adapted [13].

Although its great availability, biodiesel production from edible oils causes prices to rise in the food industry, thus aggravating criticism whether to convert these oils into biofuel instead of nourishment. The use of non-edible oil has also been in question since it also needs land and water to grow, consequently taking up space from food cultivation [17].

One of the alternatives is to grow microalgae for fuel production due to its photosynthetic efficiency in labs and its high lipid content [18]. But the difficulty of microalgae large scale production makes it hard to simulate lab conditions. Studies have shown that waste cooking oils are the best feedstock due to their availability, high free fatty acids content and their low price [19].

2.1.1 Waste cooking oil

WCO properties vary depending on its composition, being a combination of cooking oils like soybean, palm, sunflower, and canola oil. Its consumption is warned against since it can cause cancer. In Brazil, only 2 % of the disposed cooking oil is recovered and recycled and the rest of it is incorrectly discarded [20]. This waste has higher free fatty acid and water content than crude oil, which may cause saponification and hydrolysis during biodiesel production, these result respectively in loss of biofuel during phase separation and undesired product conversion into free fatty acids (FFAs). Also, water may originate separation in biodiesel/diesel blends [21].

Ravelo and Rodriguez (2018) [21] studied if the number of times the oil is used alters the properties of the resulting biodiesel through a single transesterification producing methanolic esters using KOH as catalyst. Results showed that this reaction is a suitable method for biodiesel production and that WCO meets biodiesel quality standards.

2.2 BIODIESEL PRODUCTION

The use of vegetable oil directly in the engine causes problems such as carbon deposit, corrosion, failure of engine lubricating oil, and so on. The main issue is the viscosity of the oil, whereas biodiesel is less viscous than crude oil. Therefore, there are several methods of obtaining biodiesel and lowering oil viscosity, such as pyrolysis,

esterification, and transesterification. The following topics present more details of each reaction type.

2.2.1 Pyrolysis

This method consists of heating natural oils to transform this organic matter into esters. Although it appears relatively simple, great amounts of heat must be used in this process, and it has high costs due to the complexity of equipment. In addition, the resulting product is of short-chain molecules, and it does not have the necessary fuel properties [22].

2.2.2 Esterification

The esterification process happens when a long chain free fatty acid reacts with a short chain alcohol using a homogeneous acid catalyst which forms ester and water. Biodiesel is commonly produced through this method using H_2SO_4 , HCl and H_3PO_4 as catalysts, however, great amounts of acid are necessary, along with energy demand and high cost [23]. Figure 2 shows the general esterification reaction.

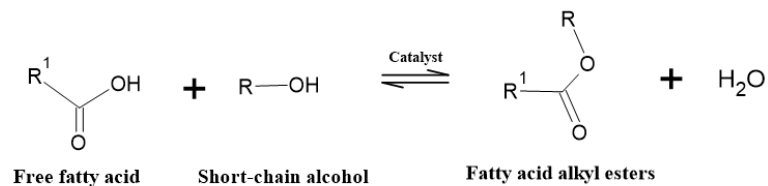


Figure 2: Esterification reaction.
Source: Adapted from [24].

2.2.3 Transesterification

Transesterification is similar to esterification as it consists in mixing triglycerides with a short-chain alcohol forming ester. For this reason, these kinds of reactions are classified as alcoholysis for they consist of the cleavage by an alcohol [16]. Transesterification is the most used reaction for biodiesel production and differs from esterification as the side product is glycerol, shown in Figure 3. For this process, alkaline metal hydroxides are more effective catalysts, and their rate is approximately 4000 times

faster than using acid catalysts. Methanol is the most used alcohol due to its hydrophilic properties, which helps to separate glycerol from biodiesel [23]. However, it has many downsides to its use: it is derived from fossil fuels, highly toxic to human health, low solubility, etc. Ethanol has been shown as a better alternative for its lower toxicity, better solvency properties, and some of the organic matters from which it can be obtained are corn, sugar cane, cassava, and potatoes. Sugarcane can grow both in tropical and subtropical climates and is the main feedstock in Brazil and other emerging countries [25].

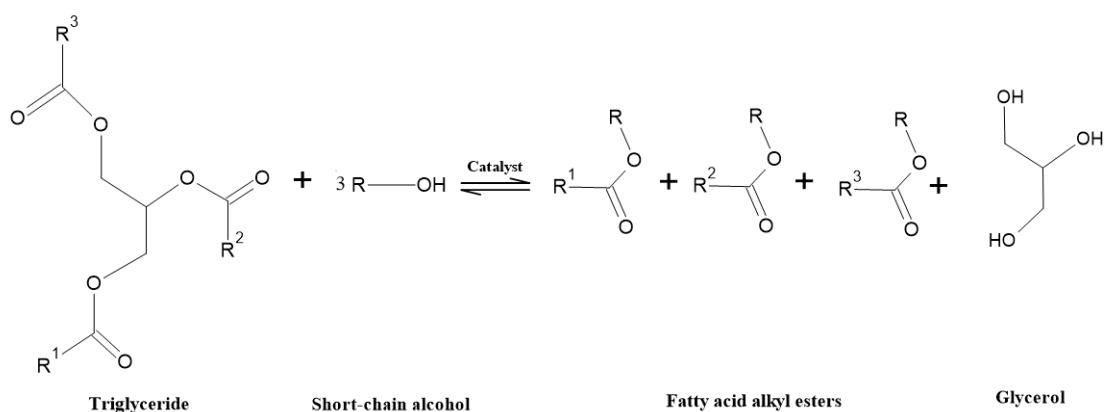


Figure 3: Transesterification reaction.
Source: Adapted from [24].

2.3 CATALYST

As mentioned before, transesterification occurs by mixing oil and alcohol. The addition of a catalyst to the mixture considerably increases the reaction rate, thus achieving equilibrium faster and a higher yield. There are many possible catalysts to be used and the main ones are classified as homogenous, heterogenous, and enzymatic.

Homogeneous catalysts have many advantages, such as high selectivity, reaction rate, turnover frequency, and some of the most used are KOH, NaOH as basic homogeneous catalysts and H₃PO₄ as acid catalyst in transesterification [26]. Alkali reactants are 4000 times faster in transesterification than acid chemicals, and among them sodium hydroxide is preferred due to its higher solubility, low cost and a low quantity is needed compared to potassium hydroxide [16, 27, 28]. However, this kind of catalyst in contact with reactants form a mixture of uniform appearance and must be separated by chemical reactions [29].

Heterogeneous catalysts, on the other hand, are composed of a solid support with alkaline or acid chemicals on its surface and favor both esterification and transesterification with oils containing high FFA and water content, besides having an easy mechanical recovery. The main representatives are alkaline metal oxides, such as CaO, CaTiO₃, CaMnO₃, among others [28, 29].

Enzymatic catalysts like lipases show high biodiesel yield, are favorable in oils with high FFA and water content and have low cost [30]. However, excess alcohol can cause denaturation and dehydration in this enzyme thus inactivating it [31]. Also, the amount of catalyst used in reactions can influence conversion into esters, forming undesired side products, such as soap [29].

Table 4 compares different studies of biodiesel production, the catalysts used and reaction conditions. Among these experiments, homogeneous basic catalysts presented a low reaction time, between 30 and 60 minutes, low amount of catalyst and high reaction yields (93.6 to 99.2 %). The downside is that these reactions demanded great alcohol:oil ratios (7.5:1 to 9:1). As for heterogeneous and enzymatic catalysts, these presented high biodiesel yields, however the first one required higher temperature, between 50 and 80 °C, and the last one also demanded long periods of reaction time (1 to 5 h). Therefore, in addition to the high yield, reactions using homogeneous catalysts consumed less energy and, consequently, offered more favorable conditions for large scale production.

Table 4: Catalysts used in biodiesel production and yield through transesterification.

Catalyst type	Catalyst	Feedstock	Alcohol	Alcohol:oil molar ratio	Reaction temperature (°C)	Reaction time	Amount of catalyst (wt%)	Biodiesel yield (%)	Source
Homogeneous	NaOH	Canola oil	Ethanol	7.5:1	45	1 h	1	93.6	[32]
	KOH	Chrysophyllum albidum seed	Methanol	9:1	65	40 min	1	99.2	[33]
	KOH	Castor seed oil, waste fish oil	Methanol	8:1	32	30 min	0.5	95.2	[34]
Heterogeneous	LaTiO ₃	Wild mustard seed oil	Methanol	4:1	80	1 h	5	90.0	[35]
	CaO	Moringa seed oil	Methanol	6:1	50 – 70	2 h	3	82.7	[36]
	Bentonite zeolite/NaOH	Soybean oil	Methanol	7.47:1	57.8	1 h	1.76 and 0.77	98.6	[37]
Enzymatic	Lipase	Waste cooking oil	Methanol	4:1	40	3 h	0.05	96.0	[38]
	Lypozyme	Sunflower oil	Ethanol	3:1	50	1 h	0.08	83.0	[39]
	<i>P. fluorescens</i>	Sunflower oil	Ethanol	3.6:1	45	5 h	10	82.0	[40]

2.4 PURIFICATION

After transesterification is complete and conversion has reached its maximum capacity, the result of the process is a mixture that after decantation separates into two phases: polar and apolar. The polar phase is rich in glycerol and contains excess alcohol, catalyst, water, and impurities, while the apolar phase is rich in esters [41]. Due to density difference, biodiesel rich phase settles on top while the glycerol rich phase settles on the bottom.

One of the factors that influences purification is excess alcohol in the mixture because it has both polar and apolar properties, mainly ethanol due to its larger carbonic structure than methanol. Gomes *et al.* (2011) [32] previously evaporated ethanol from the mixture to reduce miscibility of glycerol in biodiesel.

After evaporation and decantation, the lighter phase still presents glycerol as the main contaminant and causes damage to combustion motors and the maximum free glycerol concentration allowed in biodiesel is 0.02 wt%, according to ASTM D6751 (2002) [42]. Therefore, other forms of purification are necessary, among which are membrane filtration, centrifugation, wet washing, and dry washing [41].

2.4.1 Wet washing

This is the conventional method used by industries in large scale production since alcohol, glycerol and other impurities interact with water whereas biodiesel doesn't. It also eliminates soap that may have formed during transesterification reaction [43]. It consists in the addition of distilled or acidulated water (in case of an alkaline catalyst) to the mixture post decantation up to 8 times to reach a certain purity [44]. Even though it is a simple method of purification, there are still some disadvantages, which are: a large amount of water is needed, big tanks are required for settling, long periods of time to ensure separation, and to remove residual water from the final product it is necessary great amounts of energy for its drying, thus increasing cost [2].

2.4.2 Centrifugation

Centrifugal reactors promote a speedier separation between liquids of different densities. While it increases mixing of immiscible liquids enhancing reaction efficiency,

it also decreases the time required for separation. This equipment serves as a reactor, and it is easy to scale up [6].

2.4.3 Membrane filtration

This method has been studied in recent years as it works according to the size exclusion principle. It is a selective layer that retains larger molecules and allows others to permeate [45]. Glycerol and soap, being the main contaminants in this kind of biofuel, have larger molecules than esters, and therefore are effectively retained by the membrane. Studies show that the use of membranes reduces water consumption, effluent generation, and results in a high-quality product. This process also excludes the need of previous decantation. Gomes *et al.* (2015) [46] demonstrated through experiments that a small water addition to the mixture is enough to form agglomerates and decreases glycerol permeation in the final product.

2.4.4 Dry washing

Dry washing consists of using solids with porous particles on which impurities are adsorbed. This material's surface has acidic and basic sites that interact with polar substances, like glycerol and alcohol. Commercial adsorbents are most common, such as Magnesol®, but recent studies show that naturally porous agroindustrial waste materials are very effective in biodiesel purification and have low cost compared to the one mentioned previously [4]. This process also decreases water consumption in the purification step and is environmentally friendly [47]. This topic will be further discussed in the next item in this work. Table 5 compares the purification methods according to purification conditions and glycerol removal.

Table 5: Comparison of biodiesel purification methods.

Purification method	Purification conditions	Temperature (°C)	Glycerol removal (wt%)	Source
Wet washing	Three washing steps, 10 (v/v) % acid water with 2 % H ₃ PO ₄	55	96.2	[48]
	Three washing steps, oil:water mass ratio 1:1	50	99.3	[49]
Membrane filtration	Polyvinylidene fluoride membranes, 0-0.75 wt% water addition	28	92	[50]
	Adsorbent concentration on 40 g/L, polymeric membrane, 0.2 % of added acidified water	45	72.2	[51]
Centrifugal separation	Continuous centrifugal contactor separator, 10 Hz frequency, 0.8:1 water/biodiesel ratio	35	-	[6]
	Cylindrical bowl centrifuge, 2100 rpm	-	91.4	[52]
Dry washing	Raw sugarcane bagasse, 3 wt%, 2 h batch reaction	30	82	[49]
	Magnesol, 1 wt%, batch reaction	65	-	[48]

The purification studies mentioned in the Table above presented different free glycerol removal rates. Wet washing may have had the highest rates, but the alternative methods also presented favorable results, besides being effective in lower temperatures.

2.5 ADSORPTION

Adsorption is a mass transfer process which studies the capacity of certain solids in concentrating existent substances in gaseous or liquid fluids on their surface. This allows the separation of the components in the fluid. In other words, adsorption consists of a solid capable of retaining molecules on its exterior. The solid is called adsorbent and the substances are called adsorbates [53, 54].

This mechanism is due to physical or chemical interactions, where physical interactions are weaker and attributed to Van der Waals forces, similar to molecular adherence forces. Chemical interactions, on the other hand, involve the exchange of electrons between adsorbent particles and adsorbate molecules, therefore, it is stronger. Also, chemical adsorption is more specific and occurs in certain places called active sites while physical adsorption happens all over the solids surface [53].

2.5.1 INFLUENCING FACTORS

Since adsorption occurs through physical and chemical interactions between the solid and fluid components, some of the influencing factors in this process are adsorbent and adsorbate properties. Adsorbent characteristics include surface area, pore size and functional groups on its surface. Adsorbate properties depend on its polarity, molecule size, solubility, and pH [53].

2.5.1.1 Surface area

Adsorption is proportional to the surface area per mass unit, called specific surface area, which is increased when the particle size is reduced. This also gives access to its internal pores by the fluid in contact. Therefore, the bigger the particle, the lower the specific surface area, less adsorbate enters in contact with the surface and less adsorption occurs [53].

A study developed by Wu *et al.* (2020) [54] explored the factors that influence the adsorption of polyfluoroalkyl substances in aquatic matrices. Evidently, the larger the particle, the higher the removal. This is due to an increased specific external surface area or possibly more active sites being accessed.

2.5.1.2 Temperature

The temperature in which the process occurs influences the adsorption rate constant, since heat increases the kinetic energy and consequently increases the mobility of fluid particles. A greater agitation of molecules improves diffusion into the adsorbent's pores. Higher temperatures also lower fluid viscosity and help intraparticle diffusion [53, 55].

In their studies, Paschoal *et al.* (2023) found that temperature has a great influence on glycerol removal from crude biodiesel using passion fruit seed without activation. In a 30 °C adsorption process, the removal of adsorbate was 42.7 % while at 45 and 60 °C the removal was 72.9 and 77.1 %, respectively. This relates to a more effective diffusion rate of the solution in the adsorbent pores [51, 56].

2.5.1.3 pH

The pH level plays a significant role in determining the adsorption behavior of chemical species onto adsorbents. It affects the surface charges of the adsorbent and the ionization of the adsorbate, ultimately influencing the adsorption capacity and efficiency. The point of zero charge (pH_{PZC}) is an index that indicates whether a surface becomes positively or negatively charged as the pH changes. For pH lower than pH_{PZC} the surface is positively charged, and higher pH causes a negatively charged surface [53].

Nizam *et al.* (2021) [57] studied the influence of pH on removal of dyes from aqueous solution using biomass-based powdered activated carbon (PAC). It was observed that at higher pH there was a decrease in charge and consequently lower dye removal, whereas negatively charged PAC increased ionization rate of the adsorbate.

2.6 ADSORBENTS

Considering the adsorption influencing factors and the solution from which a component is to be removed, the choice of adsorbent is very important. The desired physicochemical properties depend on the purpose of the process, it may help to remove a contaminant or to concentrate a desired substance. If the goal is to recover the substance, it is best if the interactions are weaker and easier to reverse, whereas for the removal of an undesired component, they may not need to be as specific or reversed. The most used adsorbents are silica-based materials and activated carbon.

Silica materials are industrially produced and can cause damage to the environment if incorrectly disposed of. Studies show that some kinds of biomass are also highly porous carbon-based materials with large surface area treated to serve as adsorbent. They can be carbon rich organic substances and have great potential for glycerol removal. Table 6 shows some recent studies with biomass adsorbents and their results in biodiesel purification.

Table 6: Biomass as adsorbent and its effect in biodiesel purification.

Adsorbent	Feedstock	Amount of adsorbent (wt%)	Temperature (°C)	Free glycerol removal (wt%)	Source
Potato starch	Sunflower oil	5	25	100	[46]
Corn starch	Sunflower oil	10	25	95.3	[46]
Cassava starch	Sunflower oil	1	25	100	[46]
Cellulose	Sunflower oil	10	25	100	[46]
Sugarcane bagasse	Soybean oil	3	30	82	[48]
Nutshell	Waste cooking oil	5	15	56.3	[1]
Sawdust	Waste cooking oil	5	15	54.8	[1]
Coconut coir	Waste cooking oil	5	15	33.3	[1]
Rice husk	Waste cooking oil	5	15	32.1	[1]
Olive pits	Waste cooking oil	5	-	82.7	[58]
Cork powder	Waste cooking oil	2	25	89	[59]

Activated carbon is produced by carbonizing biomass at high temperatures altering the superficial properties of the adsorbent and significantly increasing surface area and therefore, adsorption capacity. González *et al.* (2007) [60] studied different procedures to enhance avocado kernel seeds surface area and the results are shown in Table 7. The natural kernel had a low specific surface area (53 m²/g) and the different types of activation had positive effects in improving it, especially with H₃PO₄ activation and carbonization at 800 °C (1802 m²/g).

Table 7: Adsorbents preparation and specific area.

Adsorbent code	Sample description	Specific area (m ² /g)
AGAP	Natural, without activation and carbonization	53
AGAP1	Activated with peroxide	29
AGAP-800	Carbonized at 800 °C	227
AGAP-1000	Carbonized at 1000 °C	452
AGAP-P-800	Activated with H ₃ PO ₄ and carbonized at 800 °C	1802
AGAP-P-N-800	Activated with H ₃ PO ₄ and carbonized under nitrogen flow at 800 °C	1590

Source: [60].

2.7 KINETICS

Adsorption kinetics are measured through mass transfer between fluid and adsorbent over time. Therefore, the component in the solution in contact with the adsorbate is transferred to the surface and inner pores of the solid particles and the speed of this process is observed. It can be affected by temperature, pH, ionic forces, adsorbate initial concentration, agitation, size of the particles and pore size distribution. Lastly, it is graphically represented by adsorbate concentration in the solution over time [53].

This study can be used to determine the moment in which the adsorption reaches equilibrium, as well as the best temperature by evaluating glycerol removal. Several models are used to study the behavior of the experimental data, such as pseudo-first and pseudo-second order models represented by Equations 1 and 2, respectively.

$$q_t = q_e[1 - e^{-k_1 t}] \quad (1)$$

$$q_t = q_e - \frac{q_e}{q_e k_2 t + 1} \quad (2)$$

q_t : adsorbate concentration removed by the adsorbent (mg/g).

q_e : mass of adsorbate removed by the adsorbent at equilibrium (mg/g).

k_1 : pseudo-first order constant (min^{-1}).

k_2 : pseudo-second order constant [$\text{g}/(\text{mg}\cdot\text{min})$].

t : reaction time (min).

2.7.1 Activation energy

The kinetic data at different temperatures can be used to determine the activation energy needed for this adsorption process and its magnitude may indicate if the adsorption is of chemical or physical interaction. Physical interactions reach equilibrium faster for the energy needed is lower ($E_a < 4.2 \text{ kJ/mol}$) whereas chemical interactions take longer due to the higher energy required ($8.4 \text{ kJ/mol} < E_a < 83.7 \text{ kJ/mol}$) [61].

The effect of temperature over the adsorption is mainly on the kinetic constant of adsorption rate, due to the increase in kinetic energy and intraparticle diffusion rate. Moreover, temperature variation changes the adsorption equilibrium state [53].

For that, the temperatures, and the values of k_1 and k_2 were used in Arrhenius equation (Equation 3) and the result was found by linearizing this equation, shown in Equation 4, and plotting a slope between values of $1/T$ and $\ln k$.

$$k = A e^{\frac{-E_a}{RT}} \quad (3)$$

$$\ln k = \frac{-E_a}{RT} + \ln A \quad (4)$$

k: kinetic constant [min^{-1} or $\text{g}/(\text{mg}\cdot\text{min})$].

A: pre-exponential factor.

Ea: activation energy (kJ/mol).

R: ideal gas constant [8.314 J/(mol.K)]

T: temperature (K).

2.8 ISOTHERMS

Adsorption occurs until the solution's final concentration (C_e) remains constant and equilibrium is reached. At this point, it is possible to determine the adsorbent's capacity (q_e). The procedure for this experiment is to add a certain amount of adsorbent to a series of solutions with different initial concentrations of adsorbate (C_0) and a certain amount of solution (m_b), thus obtaining the adsorption isotherm. The values of C_e are obtained after a certain time by determining glycerol concentration in the solution after the equilibrium is reached, while q_e is determined through Equation 5 originated from mass conservation principle [53].

$$q_e = \frac{(C_0 - C_e)m_b}{m_a} \quad (5)$$

q_e : adsorption capacity (mg/g).

C_0 : initial adsorbate concentration in the liquid (wt%).

C_e : adsorbate concentration in the liquid at equilibrium (wt%).

m_b : biodiesel mass (g).

m_a : adsorbate mass (g).

It is graphically represented by the curves formed by q_e versus C_e as shown in Figure 4. Each of them demonstrates either extremely favorable, favorable, linear, or unfavorable adsorption. They reveal if the amount of adsorbate on the solid is higher or lower than the equilibrium concentration in the solution [53]. The isotherm models used in this work are Freundlich and Langmuir.

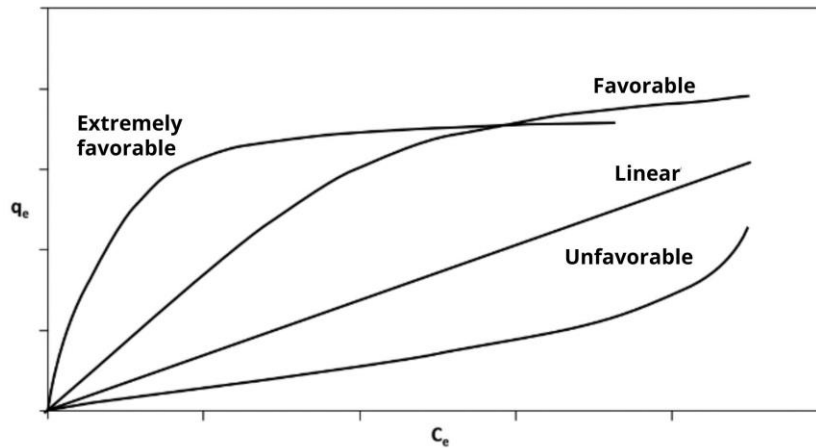


Figure 4: Isotherm typical behaviors.
Source: Adapted [53].

- Linear: the mass of adsorbate withheld per mass unit of adsorbent is proportional to the equilibrium concentration in the solution.
- Favorable and extremely favorable: the mass of adsorbate withheld per mass unit of adsorbent is higher than the equilibrium concentration in the solution.
- Unfavorable: the mass of adsorbate withheld per mass unit of adsorbent is lower than the equilibrium concentration in the solution.

2.8.1 Freundlich

The Freundlich isotherm model can be applied to non-ideal systems, on heterogeneous surfaces and multilayer adsorption. Its equation (Equation 6) is exponential and shows the different adsorption sites with different adsorptive energy.

$$q_e = K_F C_e^{1/n} \quad (6)$$

q_e : mass of adsorbate removed by the adsorbent in the equilibrium (mg/g).

K_F : Freundlich equilibrium constant (mg/g).(mg/g)^{-1/n}.

C_e : glycerol residual concentration (mg/g).

n : dimensionless exponent in the Freundlich model.

For the adsorption to be favorable, n must be a number between 1 and 10 and, the higher the value, the stronger is the interaction between adsorbate and adsorbent. If $1/n$ is

greater than 1, the adsorbate has greater attraction for the solvent and if $1/n$ is equal to 1, all the adsorption sites have the same interaction energy for the adsorbate.

2.8.2 Langmuir

The Langmuir model presents the following assumptions: there is a defined number of active sites, the sites have equivalent energy between one another, and the adsorbate particles interact only with the solid, there is the formation of a monolayer, and each active site interacts with one adsorbate molecule. This model follows Equation 7.

$$q_e = \frac{Q_{max}K_L C_e}{1 + K_L C_e} \quad (7)$$

q_e : mass of adsorbate removed by the adsorbent in the equilibrium (mg/g).

C_e : glycerol residual concentration (mg/g).

Q_{max} : maximum adsorption capacity (mg/g)

K_L : Langmuir equilibrium constant (g/mg).

2.8.3 Linear

The linear isotherm model (Equation 8) indicates that the adsorbate removed by the solid is proportional to the amount of adsorbate in the solution and doesn't indicate a maximum adsorption capacity.

$$q_t = kC_e \quad (8)$$

q_t : mass of adsorbate removed by the adsorbent (mg/g).

k : linear constant.

C_e : glycerol residual concentration (mg/g).

2.8.4 BET

The model (Equation 9) proposed by Brunauer, Emmett and Teller (BET) considers the formation of layers and the assumption that the multilayer adsorption occurs

due to condensation forces in the adsorbent's capillaries. Also, this model admits the possibility of the adsorbate layer forming new adsorption sites and consequently, new layers [53].

$$q_e = \frac{q_m K_L C_e}{(1 - K_L C_e)[1 + (K_L - K_S)C_e]} \quad (9)$$

q_e : mass of adsorbate removed by the adsorbent in the equilibrium (mg/g).

C_e : glycerol residual concentration (mg/g).

q_m : maximum adsorption for complete monolayer (mg/g)

K_L : Langmuir equilibrium constant (g/mg).

K_S : equilibrium constant for multilayer adsorption (g/mg).

3. METHODOLOGY

3.1 REACTANTS

For this study, the reactants needed were: diethyl ether from Fischer Scientific, absolute anhydrous ethanol ($\geq 99.5\%$), n-hexane ($\geq 99\%$) and hydrated ethanol 96° from Carlo Elba, phenolphthalein, potassium bromide and sodium chloride from Panreac, potassium hydroxide from Pronlab, sodium hydroxide ($\geq 98\%$), sodium periodate, hydrochloric acid ($\geq 37\%$) and acetic acid from Honeywell, ammonium acetate, methyl heptadecanoate and acetylacetone from Sigma Aldrich. Also, olive pits residue material from Casa de S. Amaro and WCO from Cantina IPB were used for adsorbent and biodiesel production, respectively.

3.2 EQUIPMENT

For biodiesel production, a heating plate from IKA (C-MAG HS4) was used followed by a rotatory evaporator (R-114) from Büchi Labortechnik AG. For the AC production, a Retsch ZM 200 Ultra Centrifugal Mill, a muffle (6000) from Thermolyne and an oven (9000) from Scientific were needed.

For biodiesel characterizations, the equipment used was a spectrophotometer V-730 from Jasco and Gas Chromatography with Flame Ionization Detector (Nexis GC-2030) from Shimadzu.

Adsorbent analyses were made using Spectrum Two FTIR PerkinElmer Spectrometer, Hanna HI2020-02 pH meter, Thermogravimetric Analyzer TGA-50 from Shimadzu and orbital incubator from Shell Lab.

3.3 WCO CHARACTERIZATION

3.3.1 WCO acidity

The oil acidity was determined according to the European Standard EN 14140:2003. In an Erlenmeyer flask, 1 g of oil was added along with 25 mL of diethyl ether 1:1, absolute anhydrous ethanol, and phenol phthalein. A standard solution of KOH was used to titrate the previous solution and acidity was calculated through Equation 10.

$$AV = \frac{V_{KOH} C_{KOH} MM_{KOH}}{m_{sample}} \quad (10)$$

AV: acid value (mg KOH/g).

V_{KOH} : volume of titrant solution (mL).

C_{KOH} : concentration of standard solution (mol/L).

MM_{KOH} : molar mass of KOH (g/mol)

m_{sample} : sample mass (g).

3.3.2 Density

A pycnometer was used first by weighing it and then adding distilled water until filled. The material was then dried and WCO was added and weighed. Distilled water is the reference liquid, and the oil is the liquid to be studied. The density is given by Equation 11.

$$\rho_{oil,water} = \frac{\rho_{oil}}{\rho_{water}} = \frac{\left(\frac{m_{oil}}{V_{pycnometer}}\right)}{\left(\frac{m_{water}}{V_{pycnometer}}\right)} = \frac{m_{oil}}{m_{water}} \quad (11)$$

$\rho_{oil,water}$: relative density between oil and water.

ρ_{oil} : oil density (kg/m³).

ρ_{water} : water density (kg/m³).

m_{oil} : oil mass (kg).

m_{water} : water mass (kg).

$V_{pycnometer}$: pycnometer volume (mL).

3.4 BIODIESEL PRODUCTION

Biodiesel production was done by previously filtering the crude WCO twice using paper filter to remove any solid contaminants in solution. In a separate container, anhydrous absolute ethanol (7.5:1 alcohol:oil molar ratio) and sodium hydroxide (0.5 wt%) were mixed until solubilization, adding this mixture to waste cooking oil preheated at 30 °C and maintaining temperature and agitation for 1 h. After transesterification, the reaction mixture went through evaporation in order to remove excess alcohol. Afterwards,

the solution was left to settle for 24 h and the phases were separated. The heavier phase rich in glycerol and impurities were removed while the lighter phase rich in esters went through a batch purification process with olive pit activated carbon (OPAC), so the final product only contains 0.02 wt% glycerol. Figure 5 shows the flowchart of biodiesel production with reactants, processes, and side and final products.

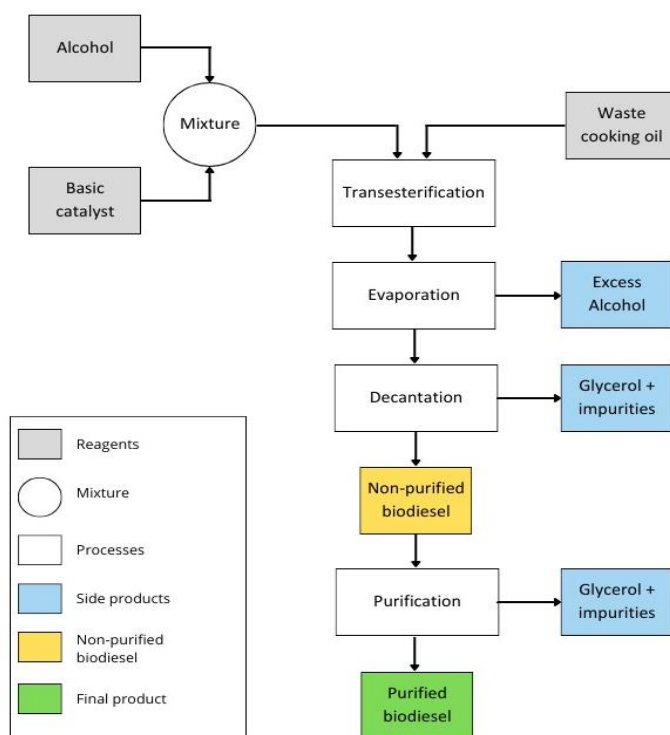


Figure 5: Biodiesel production through transesterification.
Source: The author.

3.4.1 Glycerol quantification

Glycerol was quantified using the European standards EN14105 (2020) [61], EN14106 (2003) [62], and the ASTM D6584 (2021) [63] standard but using UV/Vis Spectroscopy instead of gas chromatography. For that, three stock solutions were prepared: acetic acid solution (1.6M), ammonium acetate (4.0M), and an ethanol working solution of equal volumes of water and hydrated ethanol 96°, all using distilled water.

Other two solutions were prepared daily: acetylacetone (0.2M) and sodium periodate (10 mM). The first one was prepared by mixing 200 mL of acetylacetone in 5 mL of the acetic acid solution, and lastly 5 mL of ammonium acetate solution. The second

one was similar, 21 mg of sodium periodate dissolved in 5 mL of acetic acid solution and later in 5 mL of ammonium acetate solution.

A calibration curve was previously developed by Garção (2023) and is displayed in Appendix A [64]. For this experiment, the same conditions as the author were used. A sample of 1g of biodiesel was weighed and 4 mL of hexane and 4 mL of working solvent were added. After mixing it for 5 minutes, the solution was centrifuged for 15 min at 2100 rpm. The upper phase was then removed, and 0.5 mL of the lower phase was transferred to another vial along with 1.5 mL of the solvent. After that, 1.2 mL of the sodium periodate solution was added and mixed for 30 s. Later, the same volume of the acetylacetone solution was added and put in a 70 °C water bath for 1 min. The reaction was interrupted in a cold-water bath and read in the UV/Vis spectrophotometer at 412 nm.

3.4.2 Fatty acid ethyl ester (FAEE) yield

One of biodiesel quality standards is the percentage of FAEE's in its composition. The Gas Chromatography with Flame Ionization Detector (GC-FID) was used according to EN14214:2012 standard, which defines that the ester content must be greater than 96.5 wt% [65]. The method consists of analyzing a standard of 37 different FAME's (Appendix B) done previously by Monteiro *et al.* (2021) and comparing its peaks with the ones produced by the sample which yield is unknown [66].

In a 15 mL vial, 250 mg of biodiesel sample was added along with 5 mL of a 5mg/mL solution of methyl heptadecanoate. Anhydrous sodium sulfate was also added so the sample didn't have any water residue. The resulting solution was mixed and left to settle. Finally, an aliquot of 1 mL was inserted into a 1.5 mL vial for GC analyses. The rehearsal used the following conditions: 1 mL/min helium flow, beginning at 50 °C (1 min) and escalating at 25 °C/min until reaching 200 °C. A final ramp was used at 3 °C/min until reaching 230 °C taking 20 minutes to analyze each sample.

3.5 ADSORBENT PREPARATION

The olive pits received from Casa de S. Amaro were almost completely free of oil. Activated carbon (AC) was produced from olive pits which were ground at 12000 rpm using an opening of 250 µm until fine powder (using a Retsch ZM 200 Ultra

Centrifugal Mill) and activated physically by heating until 800 °C in a muffle for 1 h. After cooling, it was washed with distilled water and the pH was adjusted between 6 and 7 with HCl and NaOH solutions (0.02 M) and later dried one more time at 90 °C for 24 hours. The olive pits and AC were characterized according to pH_{PZC} , granulometry, FTIR, surface composition and thermogravimetry.

3.5.1 Granulometry

After grinding the dry olive pits, the particle size distribution was determined using sieves of 40, 50, 100 and 200 mesh since the previous step doesn't produce particles of the same size. The equipment was put on a vibrating base for 10 minutes and then left to settle so there wouldn't be any particles in suspension. Later, the mass of ground olive pits in each sieve was weighed and the mean Sauter (d_s) diameter was calculated using Equation 11.

$$d_s = \frac{1}{\sum_{i=1}^n \frac{x_i}{D_i}} \quad (11)$$

x_i : frequency distribution.

D_i : mean diameter held in each sieve (μm).

3.5.2 pH_{PZC}

The point of zero charge was given by preparing 11 points of 20 mL NaCl solutions 0.05 M and initial pH between 2 and 12, which were adjusted using solutions of HCl and NaOH (0.02 M). Erlenmeyer flasks containing 50 mg of AC and the resulting solutions were put in an orbital shaker at 20 °C and 150 rpm for 24 h.

At the end of this interval, the flasks were left to settle, and the final pH was then measured, and the average value was determined.

3.5.3 Fourier Transform Infrared Spectroscopy (FTIR)

For this analysis, 2 mg of adsorbent were mixed with 200 mg of KBr, and tablet samples were made to use the Fourier transform spectroscopy. The wavelengths varied between 400 and 4000 cm^{-1} .

3.5.4 Surface composition

The surface composition distributed between acid and basic functional groups was determined using the Boehm method, where the AC was left in contact in acid or basic solutions and their concentrations were measured before and after the experiment [67]. To determine the acid functional groups, 300 mg of AC and 50 mL of NaOH (0.02 M) solution were added and left in a shaker incubator at 25 °C and at 160 rpm for 24 h. The final solution was filtrated, and an aliquot of 10 mL was back-titrated with NaOH by adding excess HCl solution. The result in number of functional groups per gram of AC (mmol/g) was then calculated by Equation 12.

$$mEq\ groups = \frac{V_T N_b (V_b - V_{sam})}{V_{al} \cdot m_{sample}} \quad (12)$$

V_T : volume of the initial solution (HCl or NaOH) (L).

N_b : concentration of the NaOH solution verified through titration (mol/L).

V_b : volume used to titrate the blank solution (L).

V_{sam} : volume used to titrate the sample (L).

V_{al} : volume of the aliquot (L).

m_{sample} : sample mass (g).

The basic functional groups were similar: 50 mL of HCl were added to 300 mg of AC and left in contact in the same conditions. Later the mixture was separated and a 10 mL aliquot was titrated. The number of basic functional groups was calculated using Equation 7 but changing the order of the subtraction.

3.5.5 Thermogravimetry (TGA)

The thermogravimetric analysis was done by *Laboratório Multiusuário de Apoio à Pesquisa Apucarana Campus (LAMAP)* at *Universidade Tecnológica Federal do Paraná* using a Thermogravimetric Analyzer TGA-50 from Shimadzu using Argon as the inert gas in a flow of 50 mL/min, with a heating rate of 10 °C/min, varying from room temperature until reaching 800 °C.

3.6 ADSORPTION STUDIES

After having the final products (biodiesel and OPAC), the purification process was performed. The best conditions for adsorption were determined through kinetic and equilibrium studies varying temperature, adsorption time and AC concentration.

3.6.1 Kinetic study

In 10 Erlenmeyer flasks of 250 mL, 10 g of biodiesel were added along with 5 % (w/w) AC. The mixture was then put in a shaker incubator at 25, 35 and 45 °C and kept in constant stirring at 150 rpm. The samples were taken out of the equipment at 5, 10, 15, 30, 60, 120, 240, 480 and 1440 min and left to settle before collecting the superior part and using a syringe and 0.22 µm filters to remove AC particles. All the experiments were duplicated as well as the glycerol quantification.

3.6.2 Equilibrium study

Batch experiments were carried out in a shaker incubator at 25 °C, at 150 rpm, for 240 min. The experiments were carried out in 250 mL Erlenmeyer flasks containing 10 g of biodiesel and adsorbent concentrations of 0.5, 1, 2, 3, 4, 5, 6, 8 and 10 % (w/w). At the end of each experiment, the adsorbent was separated from the biodiesel by filtration. The final glycerol concentration analysis was performed in duplicate.

4. RESULTS AND DISCUSSION

4.1 OIL AND BIODIESEL CHARACTERIZATION

The waste cooking oil was characterized according to its acid value and relative density and the results were 0.836 ± 0.674 mg of KOH/g of crude oil and 0.921 at 20°C, respectively. The acid value was lower than the result obtained by Abdullahi *et al.* (2023) at 5.89 mg of KOH/g of sample whereas the relative density was similar at 0.928. According to the author, the limit acid value for a basic homogeneous transesterification is 2 mg of KOH/g [68]. Otherwise, biodiesel may suffer saponification, where the free fatty acids react with the basic catalyst producing soap instead of fuel forming an emulsion that may decrease purification and quality standards [69]. The biodiesel's initial glycerol content was also determined through UV-Vis spectroscopy and its value was 0.16 wt%.

4.1.1 FAEE content and reaction yield

After the GC-FID analysis was concluded, the chromatogram was extracted and displayed in Figure 6. The peaks were identified using Appendix B according to their retention time. Camilo (2023) determined the delay time between FAME and FAEE to compare these two kinds of esters [70].

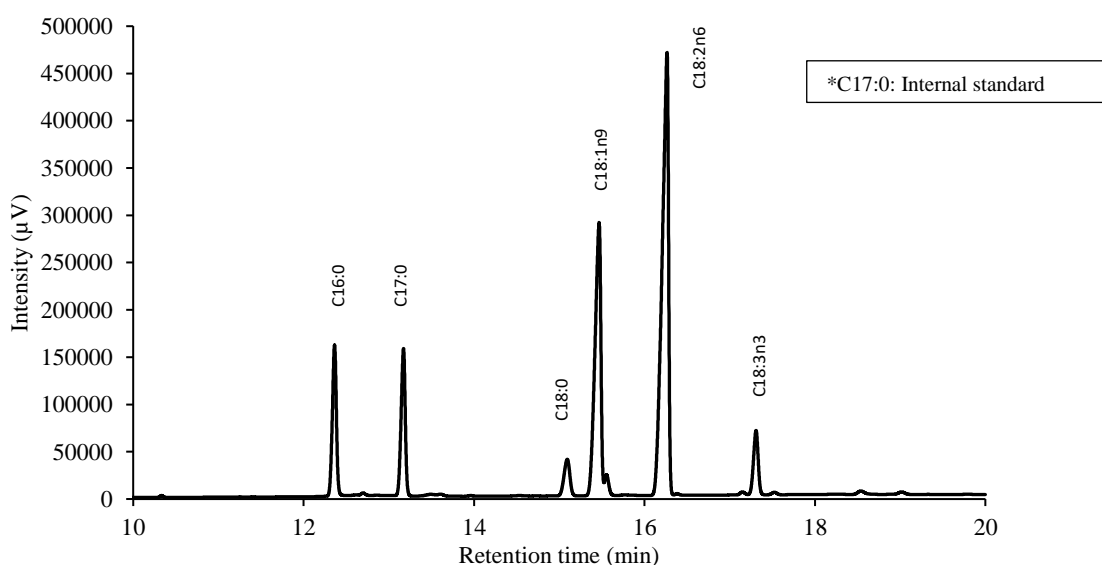


Figure 6: Biodiesel FAEE characterization.

The heptadecanoic acid methyl ester (C17:0) is the internal standard and doesn't influence the sample's mass percentage. Through the intensity of each peak and its respective retention time, it was possible to determine the FAEEs present in the biodiesel sample and consequently, in the WCO. The weight percentage of each ester is shown in Table 8.

Table 8: Methyl/ethyl esters identification in biodiesel before purification.

Retention time (min)	Peak identification		Percentage of FAEE (wt%)
12.363	C16:0	Palmitic acid ethyl ester	10.89±0.60
15.094	C18:0	Stearic acid ethyl ester	3.66±0.14
15.466	C18:1n9 (c+t)	Oleic acid ethyl ester, Elaidic acid ethyl ester	32.51±2.56
16.264	C18:2n6 (c+t)	Linoleic acid ethyl ester, Linolelaidic acid ethyl ester	47.81±1.67
17.308	C18:3n3	alpha-Linolenic acid ethyl ester	5.31±0.16
Total FAEE in the sample (wt%)			88.44±1.86

This analysis showed that 88.44±1.86 wt% of biodiesel are fatty acid ethyl esters, which was obtained through the total mass of ethyl esters in the mass of sample. This demonstrates an incomplete conversion of free fatty acids, and among these 47.81±1.67 wt% are linoleic acid methyl esters followed by oleic acid methyl esters (32.51±2.56 %). Therefore, this WCO sample was predominantly constituted of sunflower oil, commonly used in Portugal.

4.2 ADSORBENT CHARACTERIZATION

The AC's production steps are shown in Figure 7, where (a) shows the crude olive pits, which were then crushed until fine powder (b) and later carbonized at 800 °C for 1 h, had its pH adjusted and finally dried at 90 °C for 24 h (c).

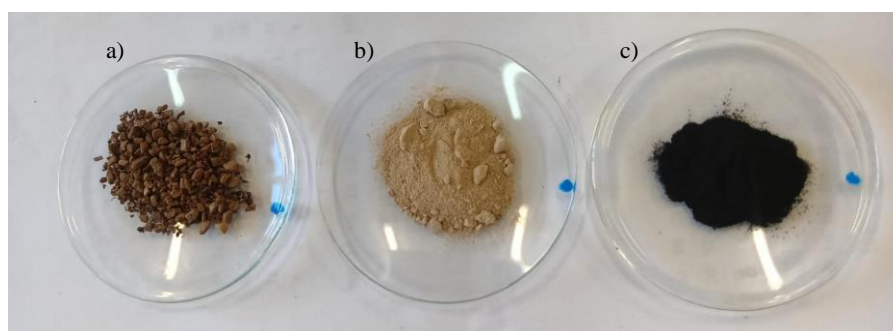


Figure 7: a) Crude olive pits, b) ground olive pits and c) OPAC.

4.2.1 Granulometry

After putting the sieves with the ground olive pits on the agitating platform, the retained weight in each one was measured, and the results are on Table 9. The resulting Sauter diameter is 0.174 mm.

Table 9: Granulometric particle size distribution.

Mesh	Diameter (μm)	Retained mass (g)	Pass accumulated	Retained accumulated
40	420	0.17	99.2%	0.8%
50	297	0.25	97.9%	2.1%
100	149	3.96	78.1%	21.0%
200	74	6.45	45.9%	54.1%
Bottom	-	9.19	0.0%	100.0%

4.2.2 pH_{PZC} and functional groups

The point of zero charge (PZC) shows that the pH of the solution in which the material is put can influence the AC's surface characteristics. For pH values lower than the PZC, the OPAC interacts with negatively charged molecules, values higher than the PZC causes interaction with positively charged molecules, and for pH equal to the PZC the adsorbent's surface is neutral [51]. The results are given in Table 10.

Table 10: AC characterization.

Sample	Yield (wt%)	pH_{PZC}	Acid sites (mmol/g)	Basic sites (mmol/g)
OPAC at 800°C	17.6 \pm 2.8	8.91 \pm 0.47	0.361 \pm 0.160	0.433 \pm 0.002

The material displayed significant weight loss after observing its yield of 17.6 \pm 2.6 %. This is due to the high temperature used, since lower temperatures display a higher yield, and due to the non-controlled atmosphere muffle. This condition may allow oxygen inside the system, thus increasing material loss.

The pH_{PZC} result (8.91 \pm 0.47) agrees with the amount of basic functional groups (0.433 \pm 0.002 mmol/g) being higher than the acid sites (0.361 \pm 0.160 mmol/g), giving it a more alkaline characteristic.

Vasques *et al.* (2013) showed that for lower pH values the removal of glycerol was greater. In this study, coconut AC had its pH changed from 9.36 to 3.35 and glycerol

removal was increased from 29 % to 83 % after a HNO₃ treatment, thus showing that the process depends on the adsorbent's pH value [72].

Still studying the adsorbent's surface composition, the FTIR analysis was used to compare the function groups before and after carbonization. The results are shown in Figure 8.

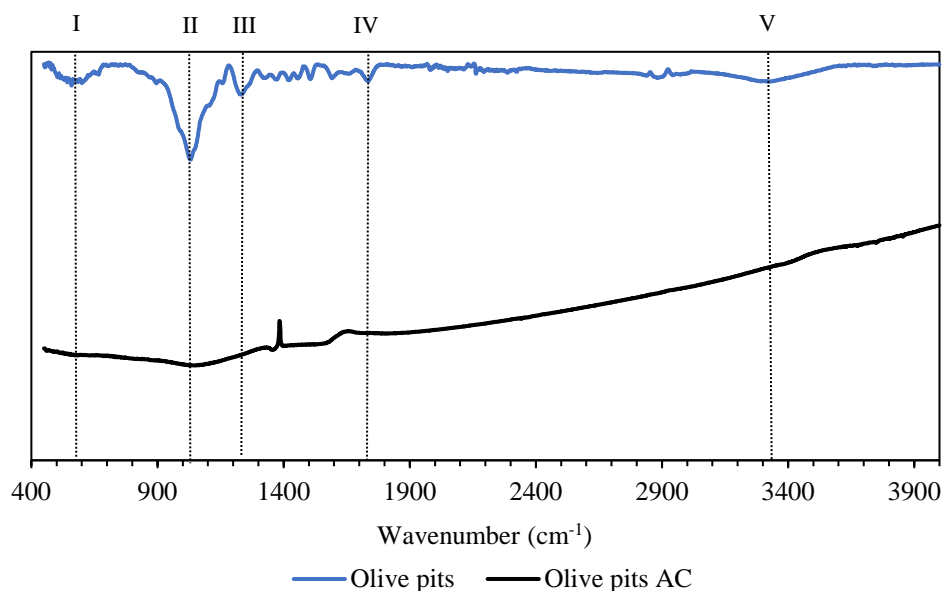


Figure 8: FTIR spectrum of olive pits before and after carbonization.

In the image above, 5 peaks are noticeable at different wavelengths and are displayed in Table 11.

Peak number	Wavenumber (cm ⁻¹)	Functional group	Reference
I	559	C-H (cyclic amides)	[73]
II	1031	C – O (alcohol and phenols)	[74]
III	1231	C = C (aromatic bond)	[57]
IV	1734	C = O (phenolic hydroxyl)	[74]
V	3323	O – H (alcohol and phenols)	[74]

The peaks mentioned in Table 11 and their respective functional groups are more noticeable on the olive pits before carbonization. After being carbonized at 800 °C the material loses its functional groups so to leave a porous material.

4.2.3 Thermogravimetry (TGA)

The thermogravimetric analysis shows the degradation of the material according to the temperature it is heated and considering the degradation time. It is studied to observe if the material is stable or if its property changes at different temperatures. For liquid surroundings and low temperatures, not much resistance is needed, unlike gaseous environments.

Figure 9 represents the behavior of the curves TG (weight *versus* temperature) and DTG (weight variation *versus* temperature). The TG curve did not show significant changes (21.85 wt%), being the first weight loss up until 90 °C where the mass difference (10.69 %) could be due to water loss. The second weight difference is between 400 and 800 °C and refers to the degradation of lignin (9.85 %) [75].

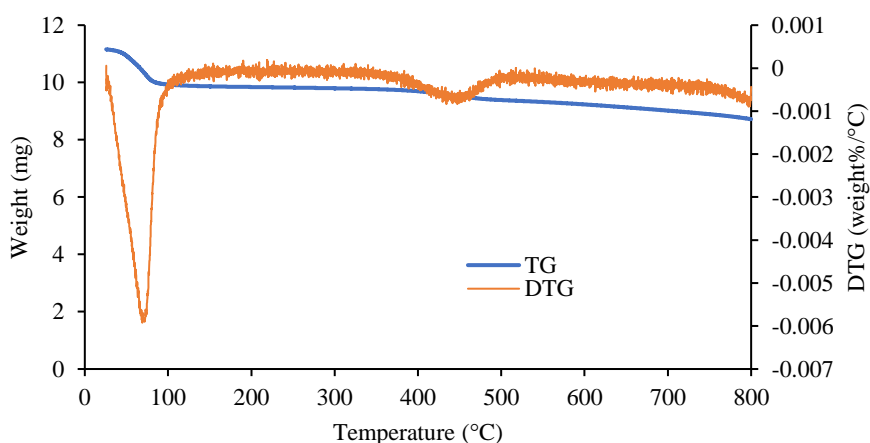


Figure 9: Thermogravimetry for OPAC.

4.3 PURIFICATION THROUGH ADSORPTION

4.3.1 Kinetics

For the kinetic study, three temperatures were chosen so to observe glycerol removal: 25, 35 and 45 °C. Figure 10 shows the percentage of glycerol removal at these temperatures and at different moments of reaction (5, 10, 15, 30, 60, 120, 240, 480 and 1440 min) maintaining adsorbent concentration at 5 wt%.

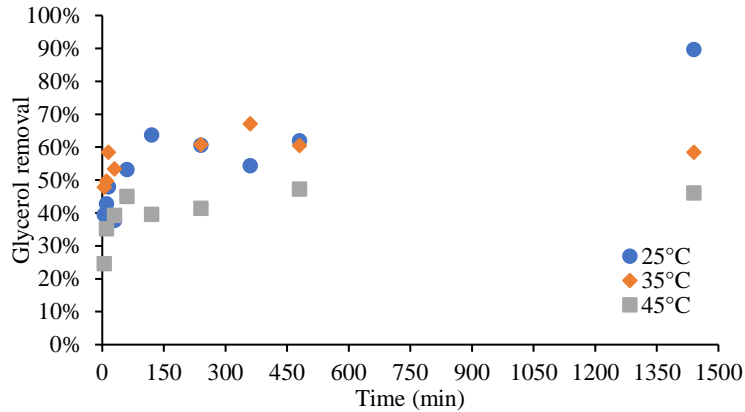


Figure 10: Kinetic study at 25, 35 and 45 °C with 5 wt% adsorbent.

With removals stabilizing at approximately 60.6, 60.8 and 41.4 % for 25, 35 and 45 °C, the equilibrium tended to be reached at 240 min for every temperature. The highest temperature was not so favorable for removal and the 25 °C and 35 °C curves showed similar glycerol removal rates.

Garção (2023) studied glycerol removal using cork and basic activated cork carbon through batch adsorption at 25, 45 and 65 °C. The author found that at low solid concentration, lower temperatures favor purification [65]. Anhesine *et al.* (2022) also observed this effect and found out that for higher temperatures, mono and diglycerol are adsorbed instead of free glycerol. Therefore, the lowest temperature was chosen for the following equilibrium isotherm study [76].

As for the glycerol content in each sample, Figure 11 shows the percentages for each temperature. The only point lower than the limit of 0.02 wt% was for 25 °C at 1440 min and the glycerol content was 0.017 wt%, which presented a total removal of 89.7 wt%.

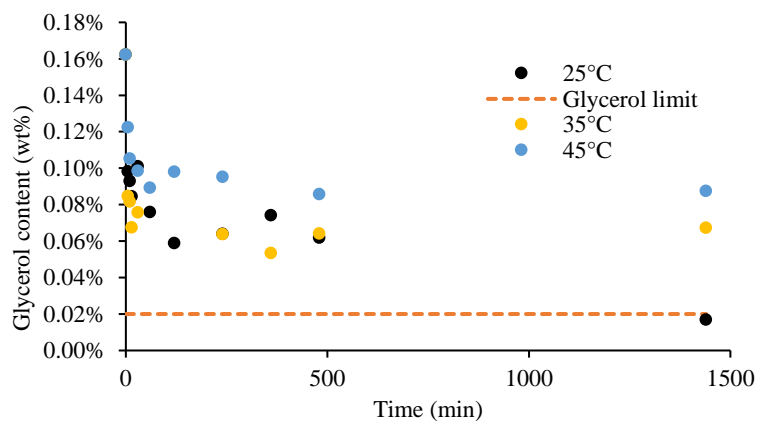


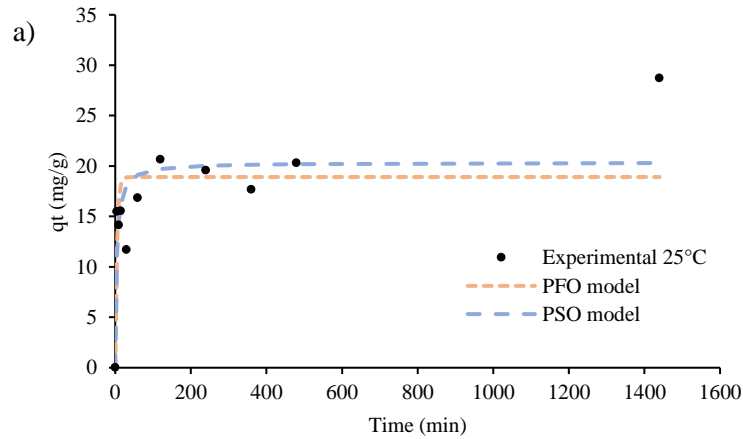
Figure 11: Glycerol content throughout the kinetic study.

Arenas *et al.* (2021) studied biodiesel purification using crude bioadsorbents, among which were sawdust, coconut coir, nutshell and rice husk dried at 100 °C in an electric oven for 3 h. The purification process happened using 5 wt% concentration of adsorbent at 15 °C. The best results were achieved when purified with sawdust and nutshell powder, with free glycerol removals of 54.8 and 56.3 %, respectively, and free glycerol content of 0.014 % [1].

The pseudo-first and pseudo-second order models were adjusted to the experimental points through the least squares method, where the error was minimized in order to find the best values for the variables k and q_e for each model. The results are shown in Figure 12 in the form of a graph of glycerol concentration on the adsorbent (q_t) *versus* time for each temperature, as well as the parameters in Table 12 used to plot the curves.

Table 12: Pseudo-first and pseudo-second order parameters for kinetic studies at 25, 35 and 45 °C with OPAC concentration equal to 5 %.

Concentration	T (°C)	Pseudo-first order			Pseudo-second order		
		k_1 (min ⁻¹)	q_e (mg/g)	Error	k_2 [g/(mg.min)]	q_e (mg/g)	Error
5%	25	0.221	18.914	181.33	0.013	20.353	139.9
	35	0.254	19.356	15.00	0.028	19.934	10.89
	45	0.160	14.156	4.88	0.018	14.701	4.03



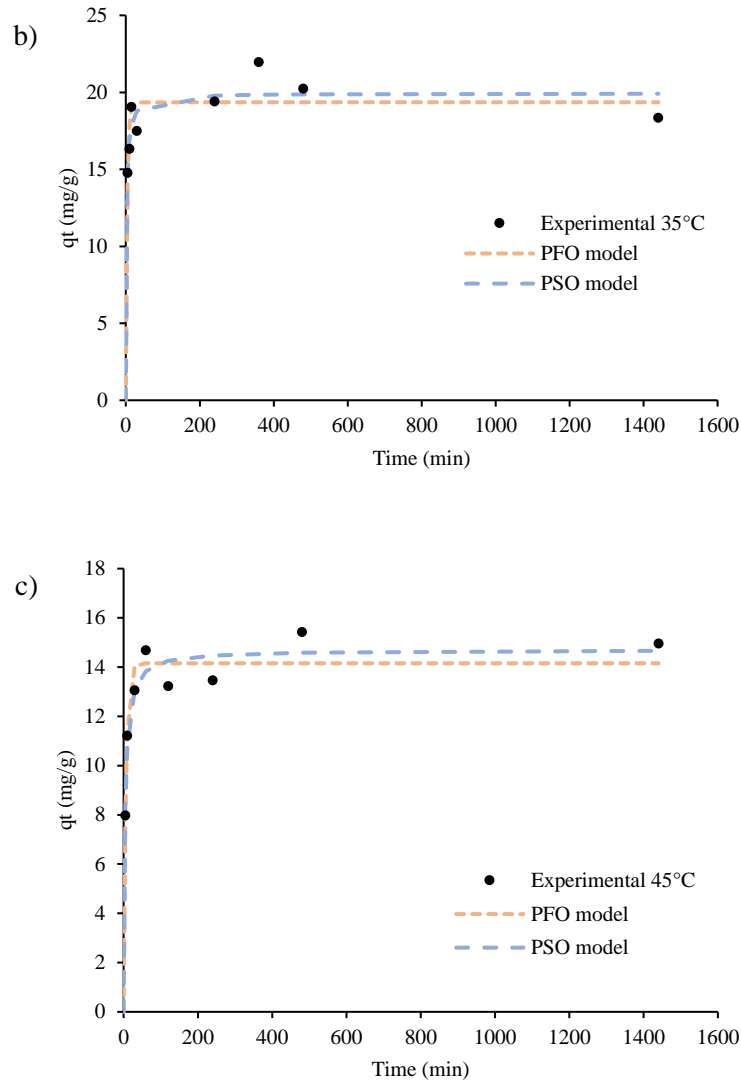


Figure 12: Glycerol concentration on the adsorbent vs time using 5 wt% OPAC at a) 25 °C, b) 35 °C and c) 45 °C using pseudo-first and pseudo-second order models.

The model with the best adjustment to the experimental data was the pseudo-second order according to the error obtained for each temperature and the greater q_e value (20.353 mg/g) of glycerol removal was at 25 °C.

4.3.2 Activation energy

The results for activation energy were obtained through the linearized Arrhenius equation (Equation 4) and are presented in Table 13. The values of pseudo-first and pseudo-second constants and their respective temperature were considered when calculating the amount of energy necessary for the adsorption to happen.

Table 13: Activation energy values for pseudo-first and pseudo-second order.

Adsorbent	Model	Ea (kJ/mol)	R ²
OPAC	Pseudo-first order	23.82	0.5040
	Pseudo-second order	88.29	0.9519

The model that best describes the adsorption of glycerol according to the Ea (88.29 kJ/mol) and R² (0.9519) values is the pseudo-second order. Therefore, it is possible to assume that the interaction between the OPAC and glycerol is mainly chemical.

4.3.3 Isotherm

After 4h of reaction, the glycerol percentage in each sample was quantified using UV/Vis spectroscopy for each activated carbon concentration. The results of glycerol percentage in the sample after purification, glycerol removal, glycerol concentration in biodiesel (Ce) and glycerol concentration on the adsorbent (q_e) are shown in Table 14.

Table 14: Glycerol content after equilibrium at 25 °C for each AC concentration.

Temperature (°C)	AC concentration (wt%)	Glycerol content (wt%)	Glycerol removal (wt%)	Ce (mg/g)	q _e (mg/g)
25	Crude biodiesel	0.1623	-	1.6227	-
	0.5	0.1486	8.44	1.4858	27.3481
	1	0.1491	8.09	1.4915	13.0610
	2	0.1344	17.19	1.3438	13.9135
	3	0.1212	25.33	1.2116	13.7748
	4	0.1003	38.21	1.0026	15.3006
	5	0.0961	40.76	0.9613	13.4931
	6	0.0886	45.37	0.8864	12.2203
	8	0.0700	56.89	0.6996	11.4955
	10	0.0394	75.70	0.3944	12.2418

The sample with least glycerol content was obtained when added 10 wt% of adsorbent to biodiesel and presented 0.0394 wt% of the contaminant and a removal of 75.70 wt%. Even though the removal was greater than observed in the kinetic study at 25 °C, after 4 h and 5 wt% of OPAC (Figure 11), the glycerol content still surpassed the established limit of 0.02 wt%. Figure 13 shows the experimental data for the equilibrium study at 25°C for each AC concentration. The point in red is the highest value for q_e obtained at 0.5 wt%.

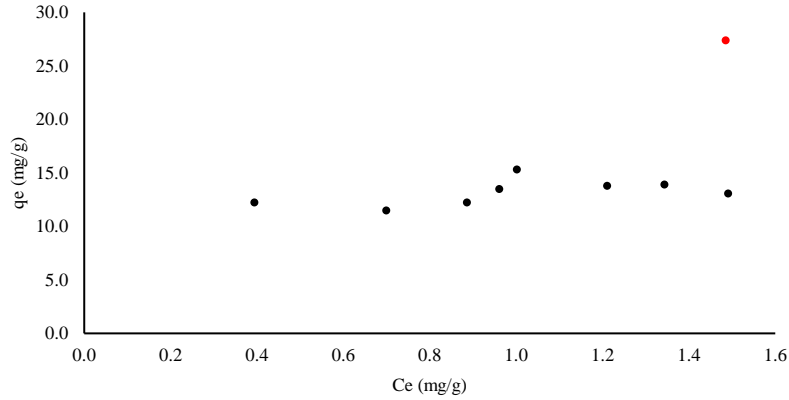


Figure 13: Isotherm experimental data at 25 °C.

Table 15 shows the parameters calculated for Freundlich, Langmuir, linear and BET models with and without the highest experimental point observed in Figure 13 for better adjustment. This was possible by minimizing the error through the total least squares method.

Table 15: Freundlich, Langmuir, linear and BET model parameters for the 25 °C isotherm.

Model	Parameter (unit)	Value (with highest point)	Value (without highest point)
Freundlich	$K_F (mg/g).(mg/g)^{-1/nF}$	14.63	13.28
	n	2.20	8.66
	Error	141.3	7.350
Langmuir	$K_L (g/mg)$	1.358	10.57
	$Q_L (mg/g)$	25.78	14.67
	Error	149.0	7.480
Linear	k	13.33	12.07
	Error	182.9	111.9
BET	K_L	10,797,447	14.65
	K_s	0.350	0.0340
	Q_{max}	8.96	13.7
	Error	126.2	7.45

Observing the error for all four models, the lowest values were found when the first point was excluded, thus having a better adjustment of the models to the experimental data. The model that best adjusted to the experimental data was Freundlich, followed by BET, Langmuir and linear due to their increasing error value.

According to the Freundlich model, n (8.66) is between 1 and 10, thus demonstrating a favorable adsorption, and a greater interaction between glycerol and AC than the interaction between biodiesel and solid. Therefore, it is possible to affirm that

the adsorption occurred in a multilayer formation and on a heterogeneous surface. Below, Figure 14 presents glycerol concentration on the liquid (C_e) versus on the solid (q_e) and the adjusted models.

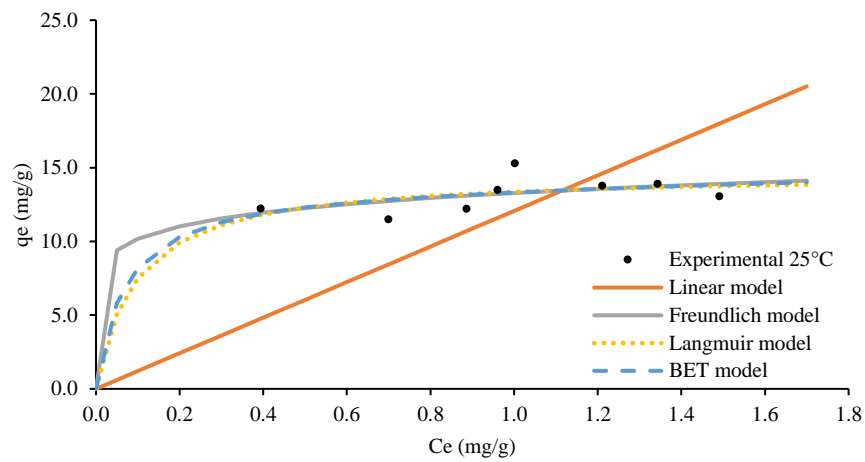


Figure 14: Isotherm experimental data at 25 °C and linear, Freundlich, Langmuir and BET models.

Freundlich, Langmuir and BET models show a favorable effect, which means that glycerol concentration on the adsorbent is higher than the equilibrium concentration in the solution. Also, equilibrium was achieved after approximately 4 h, meaning that active sites availability decreased over time.

5. CONCLUSIONS

An alternative purification method was studied so to substitute washing steps, where great amounts of water are used and later treated and discarded. The use of the olive pits activated carbon for glycerol removal and biodiesel purification was analyzed in three steps: biodiesel and AC production, characterizations, and adsorption tests.

Biodiesel was produced in different batch reactions forming one large homogeneous sample. The conditions for transesterification reaction were temperature of 30 °C, 0.5 wt% basic catalyst, 7.5:1 molar ratio of ethanol and waste cooking oil on a magnetic agitation plate for 1h. Later, the excess ethanol was removed through evaporation at 60 °C. After settling and removal of the lower phase (rich in glycerol), the unpurified biodiesel had 0.16 wt% of free glycerol, 88.44±1.86 % of fatty acid ethyl esters, which didn't achieve the amount necessary according to the norm, and 49.48±1.67 % are linoleic acid methyl esters, which concludes that the crude waste cooking oil is mostly sunflower oil.

The activated carbon was produced from dry olive pits by physical activation at 800 °C for 1 h and its carbonization yield was 17.6±2.8 wt% and had a Sauter diameter of 0.174 mm. The surface of the AC still presented basic qualities after carbonization, even though most of the functional groups were lost as seen through the FTIR analysis. The basic characteristic was shown through PZC value at 8.91±0.47 and the number of basic sites (0.433±0.002 mmol/g) greater than the amount of acid sites (0.361±0.160 mmol/g). Although, previous works show that lower PZC values favor glycerol removal.

After the thermogravimetric analysis, it was possible to see a small mass variation in the AC material, being the largest loss at temperatures lower than 90 °C, which indicates loss of water content, and the lowest mass variation at around 400 °C indicates the degradation of lignin.

The final stage of this work was to observe glycerol removal in the initial biodiesel sample and the best temperature, equilibrium time and adsorbent concentration. In order to find these conditions, kinetic studies were carried out at 25, 35 and 45 °C using an AC concentration of 5 wt% and samples were removed at different intervals between 5 and 1440 min. Glycerol concentration was determined through UV/Vis spectroscopy and the best result was achieved after 1440 min of experiment at 25 °C and presented 0.017 wt% of glycerol in the sample, with a total removal of 89.7 wt%. However, equilibrium was reached for all three temperatures after 4 h with removals of 60.6, 60.8

and 41.4 % for 25, 35 and 45 °C, respectively. Since the removal percentages for 25 and 35 °C were similar and the equilibrium was reached at 4 h, this was the chosen interval of time to carry out the equilibrium experiment and at the lowest temperature, so to lower energy consumption in large scale processes. Also, the adsorption kinetics fits a pseudo-second order behavior, with an activation energy of 88.29 KJ/mol, characterizing the interactions as mainly chemical.

The isotherm study was carried out at the conditions mentioned above (4 h and 25 °C) and varying adsorbent concentration between 0.5 and 10 wt%. According to the isotherm models used in this study, the removal showed favorable results, meaning that glycerol concentration on the solid was greater than concentration in the solution. Also, the model that best adjusted to the experimental data was Freundlich, which indicates that adsorption occurred in a multilayer formation and on a heterogeneous surface. Although the best removal of 79.70 wt% was achieved using more adsorbent (10 wt%) at the same temperature, the final glycerol content (0.0394 wt%) did not achieve the established limit (0.02 wt%).

This concludes that, in these conditions, olive pits activated carbon cannot completely substitute wet washing but does contribute to biodiesel purification through a process that does not imply the generation of large quantities of aqueous effluents.

For future steps, this study may be deepened by using different kinds of WCO with higher free fatty acid content, different activations of the olive pits so to achieve a greater glycerol removal and biodiesel purification, different conditions of transesterification so to increase ester content, repeat the adsorption process so to decrease glycerol content, observe the desorption process and reapply the adsorbent in purification, and finally, use this adsorbent in a continuous flow process through a packed column to evaluate breakthrough curve.

REFERENCES

- [1] E. Arenas, S. M. V. Cáceres, Y. R. Mejía, J. A. G. Loyola, O. Masera, G. Sandoval, Biodiesel dry purification using unconventional bioadsorbents, *Processes*. 9 (2021) 1–12. <https://doi.org/10.3390/pr9020194>.
- [2] S. Chozhavendhan, M. V. P. Singh, B. Fransila, R. P. Kumar, G. K. Devi, A review on influencing parameters of biodiesel production and purification processes, *Current Research in Green and Sustainable Chemistry*. 1–2 (2020) 1–6. <https://doi.org/10.1016/j.crgsc.2020.04.002>.
- [3] J. Milano, H. Umar, A. Shamsuddin, A. S. Silitonga, O. M. Irfan, A. H. Sebayang, I. M. Fattah, M. Mofijur, Experimental Study of the Corrosiveness of Ternary Blends of Biodiesel Fuel, *Frontiers in Energy Research*. 9 (2021). <https://doi.org/10.3389/fenrg.2021.778801>
- [4] J. M. Fonseca, J. G. Teleken, V. C. Almeida, C. Silva, Biodiesel from waste frying oils: Methods of production and purification, *Energy Conversion and Management*. 184 (2019) 205–218 <https://doi.org/10.1016/j.enconman.2019.01.061>
- [5] A. Marwaha, P. Rosha, S. K. Mohapatra, S. K. Mahla, A. Dhir, Waste materials as potential catalysts for biodiesel production: Current state and future scope, *Fuel Processing Technology*. 181 (2018) 175–186. <https://doi.org/10.1016/j.fuproc.2018.09.011>.
- [6] E. Fayyazi, B. Ghobadian, S. M. S. Ardebili, G. Najafi, S. M. Mousavi, B. H. Samani, J. Yue, Biodiesel fuel purification in a continuous centrifugal contactor separator: An environmental-friendly approach, *Sustainable Energy Technologies and Assessments*. 47 (2021) 101511. <https://doi.org/10.1016/j.seta.2021.101511>.
- [7] Data from bp Statistical Review of World Energy., (2021) <https://www.bp.com/content/dam/bp/business-sites/en/global/corporate/pdfs/energy-economics/statistical-review/bp-stats-review-2021-full-report.pdf>
- [8] European Commission, Renewable energy directive, (2022). https://energy.ec.europa.eu/topics/renewable-energy/renewable-energy-directive-targets-and-rules/renewable-energy-directive_en
- [9] European Commission, REPowerEU Plan, (2022). <https://eur-lex.europa.eu/legal-content/EN/TXT/?uri=COM%3A2022%3A230%3AFIN&qid=1653033742483>

- [10] UDOP. O Brasil faz maior exportação de biodiesel em 6 anos e meio. 13 de julho de 2022. Disponível em: <https://www.udop.com.br/noticia/2022/07/13/brasil-faz-maior-exportacao-de-biodiesel-em-6-anos-e-meio.html>. Accessed in 13 Aug. 2023.
- [11] M. Teixeira, India's ethanol program will cap future sugar exports, BMI, report says, Reuters. <https://www.reuters.com/markets/commodities/indias-ethanol-program-will-cap-future-sugar-exports-bmi-report-2023-07-10/>. Accessed in: 25 Sep. 2023.
- [12] C. Demy, Portugal's renewable energy production hit new record in 2023. Reuters. <https://www.reuters.com/business/energy/portugals-renewable-energy-production-hit-new-record-2023-2024-01-02/>. Accessed in: 15 Feb. 2024.
- [13] M. Anwar, Biodiesel feedstocks selection strategies based on economic, technical, and sustainable aspects, *Fuel*. 283 (2021) 119204. <https://doi.org/10.1016/j.fuel.2020.119204>
- [14] A. S. V. Costa, C. A. F. Pereira (2020). Análise técnico-social da produção de biodiesel no Brasil e no desenvolvimento agrícola do norte de Minas Gerais. *DRD - Desenvolvimento Regional Em Debate*. 10 (2020) 789–809. <https://doi.org/10.24302/drd.v10i0.2885>
- [15] L. Vinnichuk, E. Pogorelova, A. Dergunov, Oilseed market: global trends, *Earth and Environmental Science*. 274 (2019) 012030. doi:10.1088/1755-1315/274/1/012030
- [16] A. Demirbas, Biodiesel, a realistic fuel alternative for diesel engines, Springer, (2008).
- [17] M. Aghbashlo, W. Penga, M. Tabatabaei, S. A. Kalogirouf, S. Soltanian, H. H. Bandbafha, O. Mahiang, S. S. Lama, Machine learning technology in biodiesel research: A review, *Progress in Energy and Combustion Science*. 85 (2021) 100904. <https://doi.org/10.1016/j.pecs.2021.100904>
- [18] J. Y. Kim, J. M. Jung, S. Jung, Y. K. Park, Y. F. Tsang, K. Yi A. Lin, Y. E. Choi, E. E. Kwon, Biodiesel from microalgae: Recent progress and key challenges, *Progress in Energy and Combustion Science*. 93 (2022) 101020. <https://doi.org/10.1016/j.pecs.2022.101020>
- [19] B. H. H. Goh, C. T. Chong, Y. Ge, H. C. Ong, J. H. Ng, B. Tian, V. Ashokkumarf, S. Lim, T. Seljak, V. Jozsa, Progress in utilization of waste cooking oil for sustainable biodiesel and bio jet fuel production, *Energy Conversion and*

- Management. 223 (2020) 113296.
<https://doi.org/10.1016/j.enconman.2020.113296>
- [20] E. S. C. Freitas, L. H. Xavier, L. B. Oliveira, L. L. N. Guarieiro, System dynamics applied to second generation biofuel in Brazil: A circular economy approach, *Sustainable Energy Technologies, and Assessments*. 52 (2022) 102288.
<https://doi.org/10.1016/j.seta.2022.102288>
- [21] V. C. Ravelo, J. S. Rodriguez, Biodiesel production as a solution to waste cooking oil (WCO) disposal. Will any type of WCO do for a transesterification process? A quality assessment, *Journal of Environmental Energy*. 228 (2018) 117-129.
<https://doi.org/10.1016/j.jenvman.2018.08.106>
- [22] M. A. Bashir, S. Wu, J. Zhu, A. Krosuri, M. U. Khan, R. J. N. Aka, Recent development of advanced processing technologies for biodiesel production: A critical review, *Fuel Processing Technology*. 227 (2022) 107120.
<https://doi.org/10.1016/j.fuproc.2021.107120>
- [23] R. Ahmed, K. Huddersman, Review of biodiesel production by the esterification of wastewater, *Journal of Industrial and Engineering Chemistry*. 10 (2022) 1-14.
<https://doi.org/10.1016/j.jiec.2022.02.045>
- [24] X. Ma, F. Liu, Y. Helian, C. Li, Z. Wu, H. Li, H. Chu, Y. Wang, Y. Wang, W. Lu, M. Guo, M. Yu, S. Zhou, Current application of MOFs based heterogeneous catalysts in catalyzing transesterification/esterification for biodiesel production: A review, *Energy conversion and management*. 229 (2021) 113760.
<https://doi.org/10.1016/j.enconman.2020.113760>
- [25] H. Zabed, J. N. Sahu, A. Suely, A. N. Boyce, G. FARUQ, Bioethanol production from renewable sources: Current perspectives and technological progress, *Renewable and Sustainable Energy Reviews*, 17 (2017) 475-501.
<http://dx.doi.org/10.1016/j.rser.2016.12.076>
- [26] J. Van Gerpen, B. Shanks, and R. Pruszko, *Biodiesel production technology*, 2004.
- [27] H. Fukuda, A. Kondo, H. Noda, Biodiesel fuel production by transesterification of oils, *J Biosci Bioeng*. 92 (2001) 405-416. [https://doi.org/10.1016/S1389-1723\(01\)80288-7](https://doi.org/10.1016/S1389-1723(01)80288-7).
- [28] B. Thangaraj, P. R. Solomon, B. Muniyandi, S. Ranganathan, L. Lin, Catalysis in biodiesel production: a review, *Clean Energy*. 3 (2019) 2-23.
[doi:10.1093/ce/zky020](https://doi.org/10.1093/ce/zky020)

- [29] M. N. B. Mohiddin, Y. H. Tan, Y. X. Seow, J. Kandedo, N.M. Mubarak, M. O. Abdullah, Y. S. Chan, M. Khalid, Evaluation on feedstock, technologies, catalyst and reactor for sustainable biodiesel production: A review, *Journal of Industrial and Engineering Chemistry*. 98 (2021) 60-81. <https://doi.org/10.1016/j.jiec.2021.03.036>
- [30] L. R. Menezes, A. Hari, A. Inayat, L. A. Yousef, S. Alarab, M. Abdallah, A. Shanableh, C. Ghenai, S. Shanmugam, T. Kikas, Recent advances on biodiesel production from waste cooking oil (WCO): A review of reactors, catalysts, and optimization techniques impacting the production, *Fuel*. 348 (2023) 128514. <https://doi.org/10.1016/j.fuel.2023.128514>
- [31] F. T. T. Cavalcante, F. S. Neto, I. R. A. Falcão, J. E. S. Souza, L. S. M. Junior, P. S. Sousa, T. G. Rocha, I. G. Sousa, P. H. L. Gomes, M. C. M. Souza, J. C. S. Santos, Opportunities for improving biodiesel production via lipase catalysis, *Fuel*. 288 (2021) 119577. <https://doi.org/10.1016/j.fuel.2020.119577>
- [32] M. C. S. Gomes, P. A. Arroyo, N. C. Pereira, Biodiesel production from degummed soybean oil and glycerol removal using ceramic membrane, *Journal of Membrane Science*. 378 (2011) 453-461. doi:10.1016/j.memsci.2011.05.033
- [33] R. Kasirajan, Biodiesel production by two step process from an energy source of *Chrysophyllum albidum* oil using homogeneous catalyst, *South African Journal of Chemical Engineering*. 37 (2021) 161-166. <https://doi.org/10.1016/j.sajce.2021.05.011>
- [34] A. B. Fadhil, E. T.B. Al-Tikrity, M. A. Albadree, Biodiesel production from mixed non-edible oils, castor seed oil and waste fish oil, *Fuel*. 210 (2017) 721-728. <http://dx.doi.org/10.1016/j.fuel.2017.09.009>
- [35] S. Rezania, S. Mahdinia, B. Oryani, J. Cho, E. E. Kwon, A. Bozorgian, H. R. Nodeh, N. Darajeh, K. Mehranzamir, Biodiesel production from wild mustard (*Sinapis Arvensis*) seed oil using a novel heterogeneous catalyst of LaTiO₃ nanoparticles, *Fuel*. 307 (2022) 121759. <https://doi.org/10.1016/j.fuel.2021.121759>
- [36] Ruslan, J. Hardi, H. Sosidi, A. Ridhay, A. Y. Agus, Production of biodiesel based on moringa seed oil at varied reaction times by using CaO catalyst from chicken eggshells, *Journal of Physics: Conference Series*. 1763 (2021) 012054. doi:10.1088/1742-6596/1763/1/012054

- [37] L. Wu, T. Wei, Z. Lin, Y. Zou, Z. Tong, J. Sun, Bentonite-enhanced biodiesel production by NaOH-catalyzed transesterification: Process optimization and kinetics and thermodynamic analysis, *Fuel*. 182 (2016). <https://doi.org/10.1016/j.fuel.2016.05.065>.
- [38] E. Parandi, M. Safaripour, M. H. Abdellattif, M. Saidi, A. Bozorgian, H. R. Nodeh, S. Rezania, Biodiesel production from waste cooking oil using a novel biocatalyst of lipase enzyme immobilized magnetic nanocomposite, *Fuel*. 313 (2022) 123057. <https://doi.org/10.1016/j.fuel.2021.123057>
- [39] B. Selmi, D. Thomas, Immobilized lipase-catalyzed ethanolysis of sunflower oil in a solvent-free medium, *JAOCS, Journal of the American Oil Chemists' Society*. 75 (1998) 691-695. <https://doi.org/10.1007/s11746-998-0207-4>.
- [40] M. Mittelbach, Lipase catalyzed alcoholysis of sunflower oil, *J Am Oil Chem Soc*. 67 (1990). <https://doi.org/10.1007/BF02539619>
- [41] D. Singh, D. Sharma, S. L. Soni, C. S. Inda, S. Sharma, P. K. Sharma, A. Jhalani, A comprehensive review of biodiesel production from waste cooking oil and its use as fuel in compression ignition engines: 3rd generation cleaner feedstock, *Journal of Cleaner Production*. 307 (2021) 127199. <https://doi.org/10.1016/j.jclepro.2021.127299>
- [42] ASTM 6751:2002. Standard Specification for Biodiesel Fuel (B100) Blend Stock for Distillate Fuels.
- [43] N. F. Jariah, M. A. Hassan, Y. H. T. Yap, A. M. Roslan, Technological Advancement for Efficiency Enhancement of Biodiesel and Residual Glycerol Refining: A Mini Review, *Processes*. 9 (2021) 1198. <https://doi.org/10.3390/pr9071198>
- [44] V. Polishchuk, S. Tarasenko, I. Antypov, N. Kozak, A. Zhyltsov, A. Bereziuk, Investigation of the Efficiency of Wet Biodiesel Purification, *Web of Conferences*. 154 (2020) 02006. <https://doi.org/10.1051/e3sconf/202015402006>
- [45] A. M. Nasir, M. R. Adam, S. N. E. A. M. Kamal, J. Jaafar, M. H. D. Othman, A. F. Ismail, F. Aziz, N. Yusof, M. R. Bilad, R. Mohamud, M. A. Rahman, W. N. W. Salleh, A review of the potential of conventional and advanced membrane technology in the removal of pathogens from wastewater, *Separation and Purification Technology*. 286 (2022) 120454. <https://doi.org/10.1016/j.seppur.2022.120454>

- [46] M. C. S. Gomes, P. A. Arroyo, N. C. Pereira, Influence of oil quality on biodiesel purification by ultrafiltration, *Journal of Membrane Science*. 496 (2015) 242-249. <http://dx.doi.org/10.1016/j.memsci.2015.09.004>
- [47] M. G. Gomes, D. Q. Santos, L. C. Morais, D. Pasquini, Purification of biodiesel by dry washing, employing starch and cellulose as natural adsorbents, *Fuel*. 155 (2015) 1-6. <http://dx.doi.org/10.1016/j.fuel.2015.04.012>
- [48] C.S. Faccini, M. Espinosa Da Cunha, M. Silvana, A. Moraes, L.C. Krause, M.C. Manique, M.R.A. Rodrigues, E. V Benvenutti, E.B. Caramão, *Dry Washing in Biodiesel Purification: A Comparative Study of Adsorbents*, 2011.
- [49] M. J. Alves, Í. V. Cavalcanti, M. M. de Resende, V. L. Cardoso, M. H. Reis, Biodiesel dry purification with sugarcane bagasse, *Ind Crops Prod*. 89 (2016) 119–127. <https://doi.org/10.1016/j.indcrop.2016.05.005>.
- [50] K. Tajziehchi, S.M. Sadrameli, Optimization for free glycerol, diglyceride, and triglyceride reduction in biodiesel using ultrafiltration polymeric membrane: Effect of process parameters, *Process Safety and Environmental Protection*. 148 (2021) 34-46. <https://doi.org/10.1016/j.psep.2020.09.047>
- [51] S. M. Paschoal, J. G. Sgorlon, L. Gama, F. B. Scheufele, M. C. S. Gomes, Application of passion fruit seed meal in alternative biodiesel purification process: study of glycerol adsorption mechanism and incorporation into polymeric membrane, *Biofuels* (2023). <https://doi.org/10.1080/17597269.2023.2194117>
- [52] T. Chungcharoen, K. Netjaibun, T. Pratabkong, P. Suwannasam, W. Limmun, Effects of inner angle of bowl, flow rate and speed on the efficiency of glycerol separation from the raw biodiesel using cylindrical bowl centrifuge, *Energy Procedia* 138 (2017) 405–410. [10.1016/j.egypro.2017.10.184](https://doi.org/10.1016/j.egypro.2017.10.184)
- [53] R. F. Nascimento, A. C. A. Lima, C. B. Vidal, D. Q. Melo, G. S. C. Raulino, *Adsorção: aspectos teóricos e aplicações ambientais*, 2014.
- [54] C. Wu, M. J. Klemes, B. Trang, W. R. Dichtel, D. E. Helbling, Exploring the factors that influence the adsorption of anionic PFAS on conventional and emerging adsorbents in aquatic matrices, *Water Research*. 182 (2020) 115950. <https://doi.org/10.1016/j.watres.2020.115950>
- [55] A. Dabrowski, Adsorption: from theory to practice, *Advances in Colloid and Interface Science*. 93 (2001) 135-224. [http://dx.doi.org/10.1016/S0001-8686\(00\)00082-8](http://dx.doi.org/10.1016/S0001-8686(00)00082-8)

- [56] A. H. Jawad, A. S. Abdulhameed, L. D. Wilson, S. S. A. Syed-Hassan, Z. A. Alothman, M. R. Khan, High surface area and mesoporous activated carbon from KOH-activated dragon fruit peels for methylene blue dye adsorption: Optimization and mechanism study, *Chinese Journal of Chemical Engineering*. 32 (2021) 281-290. <https://doi.org/10.1016/j.cjche.2020.09.070>
- [57] N. U. M. Nizam, M. M. Hanafiah, E. Mahmoudi, A. A. Halim, A. W. Mohammad, The removal of anionic and cationic dyes from an aqueous solution using biomass-based activated carbon, *Scientific Reports*. (2021) <https://doi.org/10.1038/s41598-021-88084-z>
- [58] G. L. Camilo, M. C. S. Gomes, A. Queiroz, A. Ribeiro, P. Brito, Study of Biodiesel Production from Waste Cooking Oil by Ethyl Transesterification and its Purification Using Adsorption Processes, *CIEEMAT 2022*.
- [59] M. I. L. Garção, M. C. S. Gomes, A. Queiroz, A. Ribeiro, P. Brito, Biodiesel Production from Residual Cooking Oils and Purification by Adsorption Processes Based on Adsorbents of Natural Origin, *CIEEMAT 2022*.
- [60] M. P. E. Gonzáles, J. Mattusch, A. A. P. Cid, R. Wennrich, Characterization of adsorbent materials prepared from avocado kernel seeds: Natural, activated and carbonized forms, *J. Anal. Appl. Pyrolysis* 78 (2007) 185–193. <http://dx.doi.org/10.1016/j.jaap.2006.06.008>
- [61] Z. Aksu, S. Tezer, Biosorption of reactive dyes on the green alga *Chlorella vulgaris*, *Process Biochemistry*. 40 (2005) 1347–1361. <https://doi.org/10.1016/J.PROCBIO.2004.06.007>.
- [62] EN 14105:2020. Fat and oil derivatives – fatty acid methyl esters – determination of free and total glycerol and mono-, di-, triglyceride contents.
- [63] EN 14106:2003. Fat and oil derivatives - Fatty Acid Methyl Esters (FAME) - Determination of free glycerol content.
- [64] ASTM D6584:2021 (Test method for determination of free and total glycerin in B-100 biodiesel methyl esters by gas chromatography).
- [65] M. I. L. Garção, Biodiesel production from residual cooking oils and its purification through adsorption processes using activated carbon prepared from cork waste, Master thesis in Chemical Engineering – IPB, 2023.
- [66] EN14214:2012 Automotive fuels - Fatty acid methyl esters (FAME) for diesel engines - Requirements and test methods.
- [67] F. Monteiro, A. Queiroz, A. Ribeiro, P. Brito, Valorization of waste cooking oils

- through conversion processes into biodiesel catalyzed by [HMIM][HSO₄], Instituto Politécnico de Bragança, 2021.
- [68] S. L. Goertzen, K. D. Thériault, A. M. Oickle, A. C. Tarasuk, H. A. Andreas, Standardization of the Boehm titration. Part I. CO₂ expulsion and endpoint determination, *Carbon*. 48 (2010) 1252-1261. doi:10.1016/j.carbon.2009.11.050.
- [69] K. Abdullahi, S.S. Ojonugwa, A.S. Yusuff, M. Umaru, I.A. Mohammed, M.A. Olutoye, F. Aberuagba, Optimization of biodiesel production from Allamanda Seed Oil using design of experiment, *Fuel Communications*. 14 (2023) 100081. <https://doi.org/10.1016/J.JFUECO.2022.100081>.
- [70] I. Chanakaewsomboon, C.t Tongurai, S. Photaworn, S. Kungsanant, R. Nikhom, Investigation of saponification mechanisms in biodiesel production: Microscopic visualization of the effects of FFA, water and the amount of alkaline catalyst. *Journal of Environmental Chemical Engineering*, 8 (2020) 103538. <https://doi.org/10.1016/j.jece.2019.103538>
- [71] G. L. Camilo, Production of ethanolic biodiesel from waste cooking oils and purification through adsorption using olive pits based materials, Master thesis in Chemical Engineering – IPB, 2023.
- [72] É. C. Vasques, C. R. G. Tavares, C. I. Yamamoto, M. R. Mafra, L. Mafra-Igarashi, Adsorption of glycerol, monoglycerides and diglycerides present in biodiesel produced from soybean oil. *Environmental Technology*, 34 (2013) 2361-2369. doi: 10.1080/21622515.2013.770558.
- [73] A. N. A. El-Hendawy, Variation in the FTIR spectra of a biomass under impregnation, carbonization and oxidation conditions, *J Anal Appl Pyrolysis*. 75 (2006) 159–166. <https://doi.org/10.1016/J.JAAP.2005.05.004>.
- [74] F. Fadzail, M. Hasan, Z. Mokhtar, N. Ibrahim, Removal of naproxen using low-cost *Dillenia Indica* peels as an activated carbon, *Materials Today: Proceedings*. 57 (2022) 1108-1115.
- [75] S. M. Paschoal, J. G. Sgorlon, L. Gama, F. B. Scheufele, M. C. S. Gomes, Application of passion fruit seed meal in alternative biodiesel purification process: study of glycerol adsorption mechanism and incorporation into polymeric membrane, *Biofuels*, (2023) <https://doi.org/10.1080/17597269.2023.2194117>
- [76] Anhesine, M. W., dos Santos, A. V., Pozzi, A. R., Sarti, A., & Thomaz, D.. Utilização da cinza do bagaço de cana de açúcar no processo de purificação do

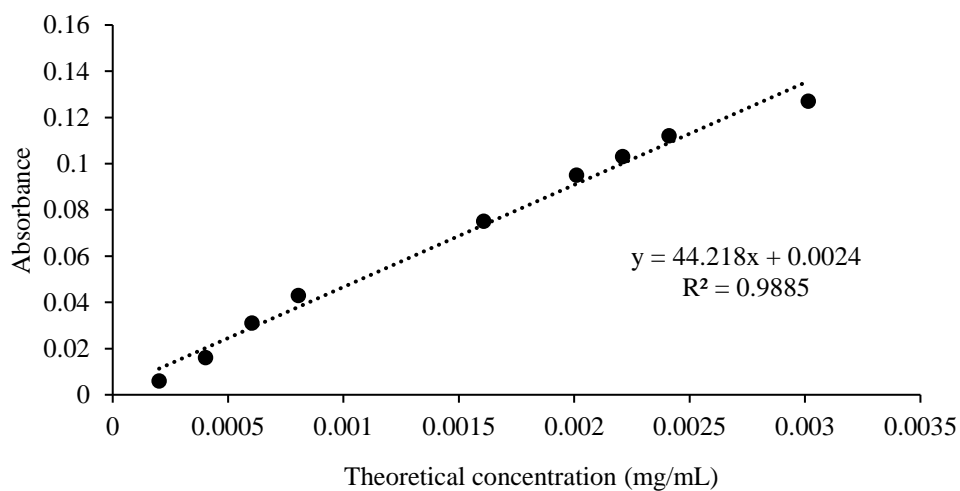
biodiesel produzido a partir de óleos e gorduras residuais. *Brazilian Journal of Development*, 8(2) (2022), 13720-13745.

APPENDIX A – CALIBRATION CURVES

Table A1 – Glycerol solutions for calibration curves.

	Glycerol volume (mL)	Solvent volume (mL)	Theoretic concentration (mg/mL)	Abs
Curve 1	0.05	3.95	2.01×10^{-4}	0.006
	0.10	3.9	4.02×10^{-4}	0.016
	0.15	3.85	6.03×10^{-4}	0.031
	0.20	3.8	8.03×10^{-4}	0.043
	0.40	3.6	1.61×10^{-3}	0.075
	0.50	3.5	2.01×10^{-3}	0.095
	0.55	3.45	2.21×10^{-3}	0.103
	0.6	3.4	2.41×10^{-3}	0.112
	0.75	3.25	3.01×10^{-3}	0.1270
Curve 2	0.8	3.2	6.43×10^{-3}	0.2225
	1.2	2.8	9.64×10^{-3}	0.4359
	1.6	2.4	1.29×10^{-2}	0.6097
	2	2	1.61×10^{-2}	0.8827
	2.4	1.6	1.93×10^{-2}	1.0275
	2.8	1.2	2.25×10^{-2}	1.2383
	3.2	0.8	2.57×10^{-2}	1.4726
	3.6	0.4	2.89×10^{-2}	1.6781
	4	0	3.21×10^{-2}	1.9068

Source: [68].



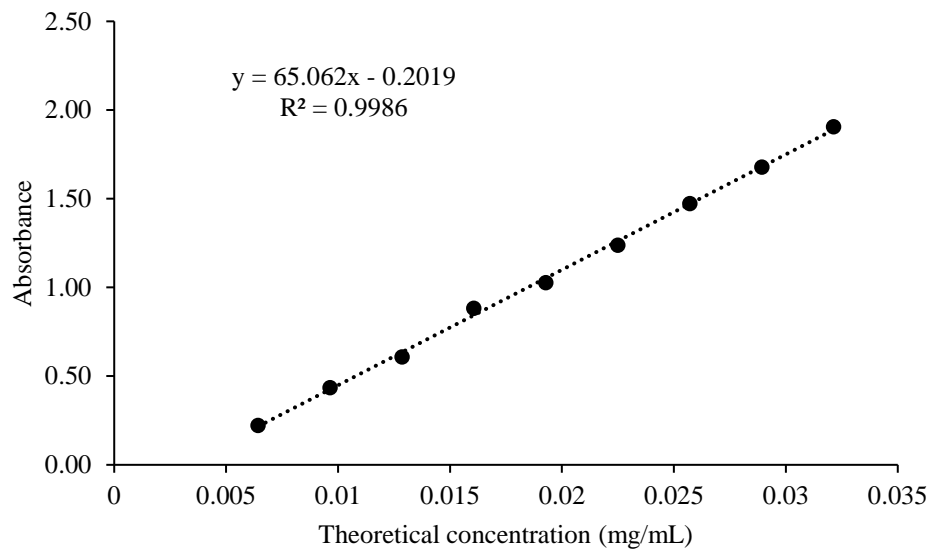


Figure A1 – Calibration curves 1 and 2.
Source: [68].

APPENDIX B – FAME IDENTIFICATION

Table B1 – Gas chromatography FAME identification.

Elution Order	Peak name	Peak ID	Retention Time
1	Butyric acid methyl ester	C4:0	4.121
2	Caproic acid methyl ester	C6:0	5.453
3	Caprylic acid methyl ester	C8:0	6.75
4	Capric acid methyl ester	C10:0	7.916
5	Undecanoic acid methyl ester	C11:0	8.507
6	Lauric acid methyl ester	C12:0	9.129
7	Tridecanoic acid methyl ester	C13:0	9.81
8	Myristic acid methyl ester	C14:0	10.584
9	Myristoleic acid methyl ester	C14:1	10.927
10	Pentadecanoic acid methyl ester	C15:0	11.482
11	cis-10-Pentadecanoic acid methyl ester	C15:1	11.889
12	Palmitic acid methyl ester	C16:0	12.536
13	Palmitoleic acid methyl ester	C16:1	12.881
14	Heptadecanoic acid methyl ester	C17:0	13.263
15	cis-10-Heptadecanoic acid methyl ester	C17:1	13.662
16	Stearic acid methyl ester	C18:0	15.177
17, 18	Oleic acid methyl ester, Elaidic acid methyl ester	C18:1n9 (c+t)	15.533
19, 20	Linoleic acid methyl ester, Linolelaidic acid methyl ester	C18:2n6 (c+t)	16.284
21	gamma-Linolenic acid methyl ester	C18:3n6	16.815
22	alpha-Linolenic acid methyl ester	C18:3n3	17.391
23	Arachidic acid methyl ester	C20:0	18.568
24	cis-11-Eicosenoic acid methyl ester	C20:1n9	19.041
25	cis-11,14-Eicosadienoic acid methyl ester	C20:2	20.118
26, 30	cis-8,11,14-Eicosatrienoic acid methyl ester, Henicosanoic acid methyl ester	C20:3n6, C21:0	20.804
27	cis-11,14,17-Eicosatrienoic acid methyl ester	C20:3n3	21.42
28	Arachidonic acid methyl ester	C20:4n6	21.776
29	cis-5,8,11,14,17-Eicosapentaenoic acid methyl ester	C20:5n3	23.311
31	Behenic acid methyl ester	C22:0	23.58
32	Erucic acid methyl ester	C22:1n9	24.332
33	cis-13,16-Docosadienoic acid methyl ester	C22:2	26.082
34	cis-4,7,10,13,16,19-Docosahexanoic acid methyl ester	C22:6n3	26.489
35	Tricosanoic acid methyl ester	C23:0	27.129
36	Lignoceric acid methyl ester	C24:0	31.664
37	Nervonic acid methyl ester	C24:1n9	32.893

Source: [69].

APPENDIX C – SCIENTIFIC PRESENTATION



PRESENTATION CERTIFICATE

This is to certify that

Camilla Groxko Smolich

presented the work

Purification of biodiesel using a natural based adsorbent in a packed-bed column

Camilla Groxko Smolich, Miriam Domingues Guimarães, João Vitor Fabian, Maria Carolina Sérgio Gomes, Ana Queiroz, António E. Ribeiro, Paulo Brito

at the XXVII Encontro Luso Galego de Química organised by the Porto Delegation of the SPQ and the Official College of Chemists of Galicia (COLQUIGA), held at Fundação Cupertino de Miranda, 22nd to 24th November 2023.

The Organizing Committee

Purification of biodiesel using a natural based adsorbent in a packed-bed column

Camilla G. Smolich^{1,2*}, Miriam D. Guimarães^{1,2}, João V. Fabian^{1,2}, Maria Carolina Sérgio Gomes³, Ana Queiroz^{1,2}, António E. Ribeiro^{1,2}, Paulo Brito^{1,2}

¹Centro de Investigação de Montanha (CIMO), Instituto Politécnico de Bragança, Campus de Santa Apolónia, 5300-253 Bragança, Portugal

²Laboratório para a Sustentabilidade e Tecnologia em Regiões de Montanha, Instituto Politécnico de Bragança, Campus de Santa Apolónia, 5300-253 Bragança, Portugal

³Universidade Tecnológica Federal do Paraná, Jardim Paraíso, 86812-460, Apucarana, Brasil

*cgroxko@hotmail.com

In Europe, the Renewable Energy Directive stimulates the development of renewable energy sources to reduce greenhouse gas emissions by at least 55% by the year 2030 and to become a climate-neutral continent by 2050 [1]. Biodiesel presents advantages over diesel fuel in terms of sulfur content, biodegradability, flash point, no aromatic content, higher cetane number and miscibility in petroleum diesel in any ratio [2].

The most used feedstock is high quality vegetable oil, but the use of waste cooking oil adds to the global reduction of residue, lower costs, and competes less for vegetable oils against the food industry [3]. This biofuel is obtained through transesterification, and glycerol is formed as a coproduct. Its presence can cause damage to motors so it must be removed until its final concentration is lower than 0.02wt%. The most used method is wet washing, but the downside is the great amount of water used and long periods of time are needed to separate biodiesel from its contaminants through decantation [4]. A promising alternative is dry washing method through adsorption using biomass activated carbon. For a more practical application, packed columns are frequently used in large scale adsorption processes. It is one of the most efficient configurations for treating great volumes of effluent and adsorption-desorption cycles [5].

For this study, crude biodiesel was produced through transesterification from a waste cooking oil sample, using ethanol and a basic catalyst (NaOH). Afterwards the biodiesel produced was characterized in terms of glycerol content. In parallel, activated carbon materials were obtained from olive pits by physical activation at 800°C. The adsorbent materials performance for glycerol removal from crude biodiesel is assessed using a continuous system based on a packed-bed column according to the following parameters: fluid rate, removal capacity, pressure drop and adsorbent recovery.

Acknowledgments

The authors are grateful to the Foundation for Science and Technology (FCT, Portugal) for financial support through national funds FCT/MCTES (PIDDAC) to CIMO (UIDB/00690/2020 and UIDP/00690/2020) and SusTEC (LA/P/0007/2021).

References

- [1] European Parliament and Council of the European Union, Renewable Energy Directive (2009/28/EC), 2018.
- [2] J.M. Fonseca et al., Energy Conversion and Management, 184 (2019) 205-218.
- [3] E. Fayyazi et al., Sustainable Energy Technologies and Assessments, 47 (2021) 101511.
- [4] S. Chozhavendhan et al., Current Research in Green and Sustainable Chemistry, 1-2 (2020) 1-6.
- [5] R.F. Nascimento et al., Adsorção: aspectos teóricos e aplicações ambientais, Imprensa Universitária da Universidade Federal do Ceará, Fortaleza, 2014.